Perspective: 2013 AIChE R. H. Wilhelm Award in Chemical Reaction Engineering

Chemical-Looping Technology Platform

Liang-Shih Fan, Liang Zeng*, and Siwei Luo
Dept. of Chemical and Biomolecular Engineering, The Ohio State University, Columbus, OH 43210

DOI 10.1002/aic.14695
Published online December 4, 2014 in Wiley Online Library (wileyonlinelibrary.com)

Keywords: carbon capture, chemical looping technology, oxygen carrier, chemical looping reactor, moving bed, chemical looping combustion, chemical looping gasification

Introduction

The term *chemical looping* was first used by Ishida et al.[1] in their description of a high-exergy efficiency combustion process that engages redox reactions that use metal oxides as reaction intermediates. The use of metal oxides as intermediates in the redox reactions as applied to processes that are noncombustive in nature can be traced to work in the early 1900s.[2,3] In this Perspective article, the term *chemical looping* is used in a broad sense to describe the nature of a reaction scheme in which a given reaction is decomposed into multiple subreactions with chemical intermediates that are reacted and regenerated.[4] The chemical intermediates considered are limited to metal oxides. Furthermore, the subreactions are ideally configured in such a manner that the exergy loss of the process as a result of this reaction scheme can be minimized. The term *technology platform* refers to a set of technologies that have been developed for various applications but share a common underlying basic concept. The concept of chemical looping is rooted in the second law of thermodynamics and applied to the reduction of the process irreversibility and, hence, the enhanced exergy efficiency of the process. The application of this exergy concept for combustion systems was reported earlier by Knoche and Richter.[5,6] Ishida et al.[1] employed metal oxides, such as NiO, CuO, Mn_2O_3, and Fe_2O_3, as chemical intermediates for combustion reaction applications. The unique feature of the use of a metal oxide in a chemical-looping combustion scheme is that CO_2 becomes an easily separable combustion product, and thus, the requirement of parasitic energy in its separation is low. Such a CO_2 separation feature has been deemed important in recent years, particularly in the consideration of global concerns over climate change.

As shown in Figure 1, growing interest in chemical looping has been evidenced by the sharp increase in the number of publications on this topic since 1994 with numbers obtained from the Web of Science. The increased interest in chemical-looping applications with metal oxides beyond combustion has also been apparent because of the potential economic benefits and commercial implications of chemical-looping processes. Specifically, the chemical-looping concept can evolve into a technology platform that yields a major impact on the formation of a variety of products that influence the fuel and chemical industries beyond the utility industry.[4,7,8]

In this article, the various types of chemical-looping reactions are described, along with the evolution of chemical-looping technology. This is followed by a discussion of the advantages of the chemical-looping scheme compared to the conventional scheme in process applications. The formulation, physical and chemical properties, morphological variations, and ionic diffusion phenomena of both the pure and composite metal oxide materials that are used as oxygen carriers are elaborated. Of equal importance to the oxygen-carrier behavior in chemical-looping technology development are the gas-solid contact pattern and the types of reactors used in the processing of these oxygen carriers. Several Ohio State University (OSU) technologies developed in recent years are introduced, and their operational efficiencies, economic impacts, and process applications are also illustrated. This article also accounts for the knowledge required for technological success, the information gap between the past and the present, and the challenges and approaches for overcoming them in the context of technology readiness, timing, and the likelihood for commercial deployment.

Two Groups of Chemical-Looping Reactions

On the basis of current applications, chemical-looping reactions with metal oxides can be categorized into two groups. Group A refers to chemical-looping reactions involving CO_2 generation or separation, as given in Figure 2(a), and group B refers to chemical-looping reactions involving non-CO_2 generation, as given in Figure 2(b). Compared to group B, group A has been studied more extensively.[4,8] Type A-I can be represented by the reactions between either metal sulfate and metal sulfide or, more typically, metal oxide and metal. In the process of the metal oxide reduction reactions that take place in the reducer or fuel reactor, the carbonaceous feedstock in gas, liquid, or solid form is fully oxidized to CO_2. The reduced metal oxide is then

**Present address:* School of Chemical Engineering and Technology, Tianjin University, China
Correspondence concerning this article should be addressed to L.-S. Fan at fan.1@osu.edu.

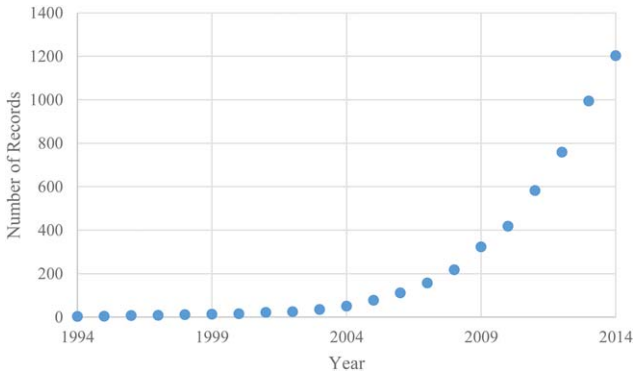

Figure 1. Cumulative number of records in the web of science containing *chemical looping* or *chemical-looping* in the topic.

regenerated in the oxidizer, combustor, or air reactor. When the reoxidizing agent is air, heat and/or electricity can be produced; when the reoxidizing agents are steam and/or CO_2, hydrogen and/or CO can be produced. The regenerated metal oxide circulates back into the reducer to complete the loop. In type A-II, the metal in the metal oxide is an alkali or alkaline earth, predominantly calcium. The type A-II reaction involves the formation of metal carbonate (e.g., $CaCO_3$) and metal oxide (CaO) through carbonation and calcination reactions, respectively. The metal oxide undergoes the carbonation reaction with CO_2 in the carbonator to form metal carbonate. Through the addition of heat in the calcination reaction, the metal oxide is regenerated from metal carbonate after CO_2 is released. The regenerated metal oxide is then recycled to the carbonator with the chemical-looping reactions repeated.

The metal oxide regeneration processes for group B reactions are similar to those for group A reactions. However, for the reduction process, they are different in that group B reactions are not intended to produce CO_2. In group B, there are three types of reduction reactions in which types B-I and B-II perform partial oxidation reactions with the carbonaceous feedstock to form syngas, a mixture of

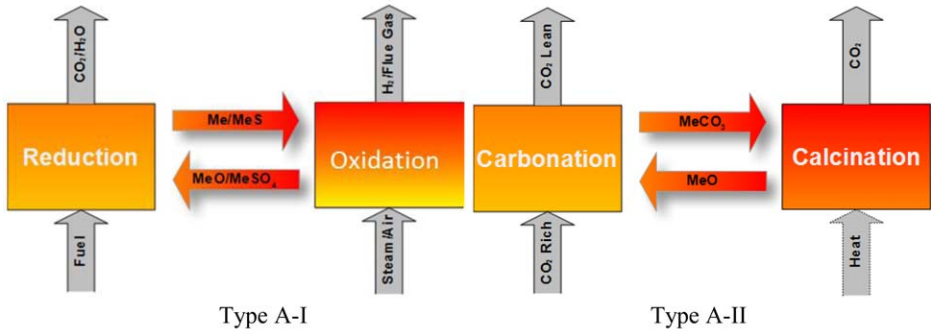

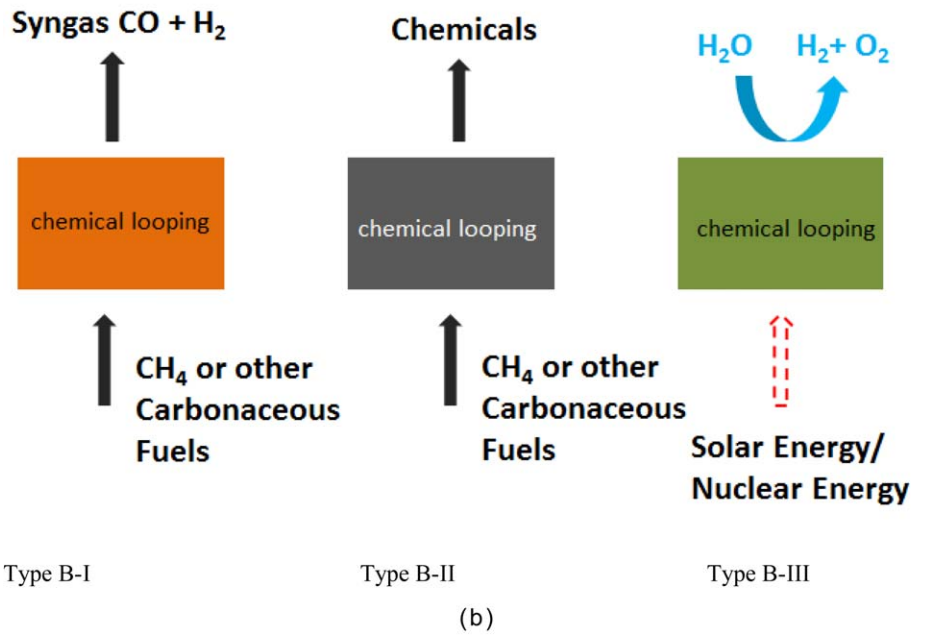

Figure 2. (a) Group A chemical-looping reactions involving CO_2 generation. (b) Group B chemical-looping reactions involving no CO_2 generation. Note: Me: metal; MeS: metal sulfide; MeO: metal oxide; $MeSO_4$: metal sulfate; $MeCO_3$: metal carbonate.

Table 1. Notable Technologies that Use the Chemical-Looping Principle

Process/developer	Lane	Lewis and Gilliland	HYGAS	CO_2 acceptor	HyPr ring
Year	1910s	1950s	1970s	1960s-1970s	1990s
Looping types	Type A-I	Type A-I, CLOU	Type A-I	Type A-II	Type A-II
Feedstock	Syngas	Solid Fuel	Syngas	Solid fuel	Solid fuel
Products	H_2	CO_2	H_2	H_2 rich syngas	H_2
Net reaction	$CO + H_2O = CO_2 + H_2$	$C+O_2 = CO_2$	$CO + H_2O = CO_2 + H_2$	$C + H_2O = CO_2 + H_2$	$C + H_2O = CO_2 + H_2$
Redox pair/looping materials	Fe_3O_4-Fe	CuO-Cu_2O or Fe_2O_3-Fe_3O_4	Fe_3O_4-Fe	$CaCO_3$-CaO	$CaCO_3$-CaO/$Ca(OH)_2$
Reactors	Fixed bed	Fluidized bed, moving bed	Two-stage fluidized bed	Fluidized bed	Fluidized bed
Gas-solid contact patterns	Gas-switching, solid fixed	Mixed/ countercurrent	Countercurrent	Mixed	Mixed
Process/developer	ARCO GTG	DuPont	Otsuka	Solar water splitting	Steinfeld
Year	1980s	1990s	1990s	1980s	1990s
Looping types	Type B-II	Type B-II	Type B-I	Type B-III	Type B-III
Feedstock	CH_4	C_4H_{10}	CH_4	H_2O	CH_4, iron ore
Products	C_2H_4	$C_4H_2O_3$	Syngas	H_2, O_2	Syngas, iron
Net reaction	$2CH_4 + O_2 = C_2H_4 + 2H_2O$	$C_4H_{10} + 3.5O_2 = C_4H_2O_3 + 4H_2O$	$2CH_4 + O_2 = 2CO + 4H_2$	$2H_2O = 2H_2 + O_2$	$4CH_4 + Fe_3O_4 = 4CO + 8H_2 + 3Fe$
Redox pair/looping materials	Supported Mn	VPO	Supported CeO_2	ZnO-Zn or Fe_3O_4-FeO/Fe	Fe_3O_4-Fe
Reactors	Fluidized bed	Fluidized bed	Fixed bed	Fluidized bed	Fluidized bed
Gas-solid contact patterns	Cocurrent	Mixed	Gas-switching, solid fixed	Mixed	Mixed

CO and H_2, and chemicals, for example, ethylene. The type B-III reaction uses heat from solar or nuclear energy to decompose the metal oxide to metal and oxygen in the reducer. The reduced metal goes to the oxidizer/combustor for regeneration to metal oxide. Water splitting to produce hydrogen can be performed when the regeneration step uses steam as the oxidizing agent. The type B-III operation shows that the chemical-looping systems can be operated in a renewable fashion without the use of fossil fuels.

Evolution of Chemical-Looping Technology

Some of the notable technology advances that use chemical-looping principles for groups A and B reactions, summarized in Table 1, are highlighted to indicate the major milestones in the development of this technology. The use of the chemical-looping concept for type A-I reactions as a technology was seen in the work of Howard Lane as early as 1904.[3,9–11] In the Lane process, shown in Figure 3, syngas derived from coal gasification was first used to reduce iron ores in a fixed bed, after which the inlet gas stream was switched to steam, and the bed then performed the steam-iron reaction to produce hydrogen. Hydrogen plants based on such a redox process were initially used to fill hydrogen balloons. They were then constructed throughout Europe and the United States to produce 24,000,000 m^3 of hydrogen annually by 1913. However, there were two major issues that hampered the efficient application of this steam-iron process: the incomplete conversion of the reducing gas and the low recyclability of the iron ores. With the availability of oil and natural gas in the 1940s, the steam-iron process for hydrogen production became less competitive and eventually phased out.

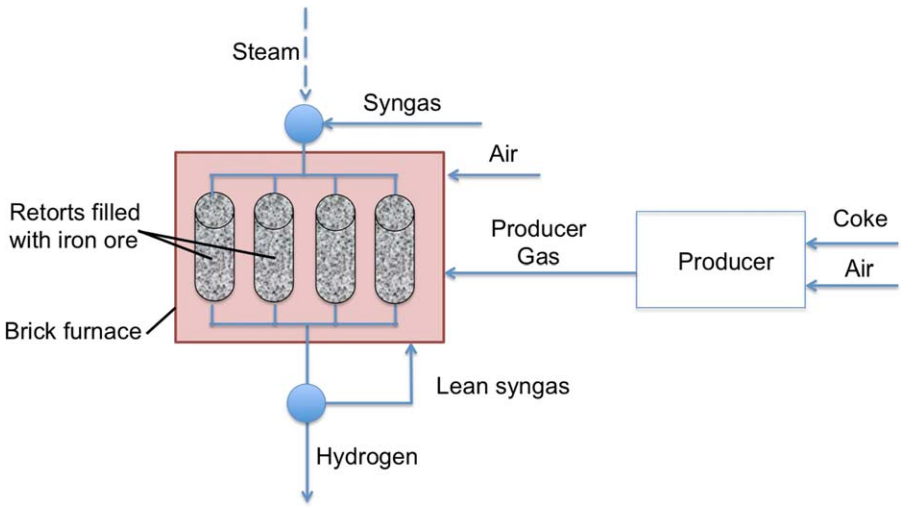

Figure 3. Steam-iron processes with a fixed bed.

In the 1950s, a type A-I chemical-looping scheme was proposed in patents by Lewis and Gilliland[12,13] with iron and copper oxides as the looping particles. The purpose of their study was to examine the feasibility of chemical looping for CO_2 generation for the beverage industry. Different types of reactors, such as fluidized beds and moving beds, were mentioned as CO_2 generators, with copper oxide as an oxygen carrier mentioned for CO_2 generation. The gas-solid countercurrent flow pattern was proposed with the iron oxide oxidation state swinging between Fe_2O_3 and Fe_3O_4.[12] Some experimental data with a small batch reactor and copper oxide were reported in their patent.[13] However, there were no published experimental data on a continuous solids flow system that substantiated the desired gas-solid contact pattern or process per se in their work. Copper oxide used as an oxygen carrier has been a focal research subject, and the copper oxide materials have been referred to as *chemical-looping oxygen uncoupling* (CLOU) materials in recent literature.[4]

In the 1970s, the Institute of Gas Technology developed the HYGAS process to convert coal and hydrogen into synthetic natural gas by a methanation reaction.[14] The hydrogen used in the HYGAS process was generated by a high-pressure steam-iron process (type A-I) with the syngas as a feedstock produced from coal gasification. Two-stage countercurrent fluidized-bed reactors were used for both the reducer and the oxidizer to enhance the fuel gas, iron oxide conversions, and mass and heat transfer. Synthesized iron oxide particles consisting of 4% silica, 10% magnesia, and 86% hematite ore were used. Both the reactivity and the strength of particles for this synthesized iron oxide were improved over the iron ore used in the Lane process. Consequently, the efficiency of the steam-iron reaction in the HYGAS process was higher than that of the Lane process. The HYGAS process was demonstrated on a pilot plant scale but was not commercialized. The drawbacks of the HYGAS process included a low metal oxide conversion, a low redox rate, and incomplete syngas conversion.

In the 1960s and 1970s, the CO_2 acceptor process (type A-II) was developed by Consolidation Coal Co. and later by the Conoco Coal Development Co., who conducted pilot-plant-scale studies.[15] In this gasifier; syngas or hydrogen was produced through the reactions of coal and steam with CaO added to the reactor to remove CO_2 and enhance hydrogen generation. Like the HYGAS process, the CO_2 acceptor process was not commercially realized, in part because of economic reasons, such as the low market price of natural gas and the high capital cost requirements for the processes. Furthermore, bituminous coals were difficult to handle, and major agglomeration problems caused by the low-temperature eutectic formation among fly ash and calcium compounds in the gasifier and the regenerator were evidenced. These could only be resolved with operational temperature and solid composition control. It was also noted that the CaS-$CaSO_4$ redox cycle observed in the CO_2 acceptor process was different from the typical redox cycles based on metals/metal oxides. According to the concept of the CO_2 acceptor process, the HyPr ring process (type A-II) was developed in Japan for hydrogen production from coal in the 1990s to 2000s.[16,17] In the HyPr ring process, more steam than that used in the CO_2 acceptor process was fed to the coal gasifier along with calcium oxide and oxygen to facilitate the capture of CO_2 by calcium oxide and to assist in the water-gas shift (WGS) reaction; this resulted in a product gas stream of about 90% H_2 mixed with methane. The solids from the gasifier consisted of mostly spent CaO sorbents ($CaCO_3$), and some unconverted carbon was introduced to the regenerator along with oxygen. The heat generated from the combustion of the unreacted carbon allowed the calcination reaction to be carried out for CaO regeneration and released a high-purity CO_2 stream for sequestration.

For group B chemical-looping reactions, in the 1980s, Keller and Bhasin produced ethylene and ethane from methane in a redox process known as *oxidative coupling of methane* (OCM).[18] In the OCM scheme, metal oxides were sequentially and separately reduced by methane and reoxidized by air. In major efforts in the adoption of the chemical-looping concept to produce chemicals en route to the production of liquid fuels via OCM (followed by oligomerization), ARCO Chemicals in the 1980s conducted research and developed a type B-II pilot-scale system using manganese composite metal oxides to convert natural gas to olefins.[19,20] In this system, low-acidity materials, such as silica, were used as supports for manganese to form braunite (Mn_7SiO_{12}) and increase the product selectivity. It was observed that the addition of alkali components such as sodium pyrophosphate further improved this selectivity. These OCM reactions took place in fluidized-bed reactors with a short gas-solid contact time, which was found to prevent further oxidation of the desired product to CO_2. The ARCO activities were halted in 1990 in part because of a lack of economic feasibility caused by the increased price of natural gas.

Maleic anhydride production from butane by vanadium phosphorous oxide (VPO; type B-II) was developed by DuPont in the 1980s and 1990s.[21] This process was developed from the bench scale to the pilot scale and, finally, to the commercial scale. Its commercial operation, however, was not successful because of the scale-up effects of the circulating fluidized-bed (CFB) reactor on the reactant contact time and the oxygen-carrier holdup in the CFB system.[22] More specifically, the insufficient oxygen-carrying capacity of the VPO particles, coupled with their attrition/breakage behavior due to the high-particle-flow requirements in the CFB system, principally contributed to the inadequacy of this process for sustainable operation at the commercial scale. The oxidation reaction of butane, thus, relied in part on molecular oxygen introduced externally. The outcome of the DuPont commercial operation underscores the importance of the viability of the oxygen carriers in CFB system operation for chemical-looping process applications.

In the 1990s, the partial oxidation of methane to syngas with CeO_2 in a type B-I chemical-looping scheme was attempted.[23] CeO_2 was found to be an oxygen carrier with a thermodynamically favored selectivity for CH_4 oxidation toward CO and H_2. Its slow kinetics and high carbon deposition properties could be resolved by the use of more sophisticated oxygen-carrier materials.[24–27] Solar-assisted metal oxide thermochemical-looping processes, which coproduced iron and syngas with the partial oxidation of methane with

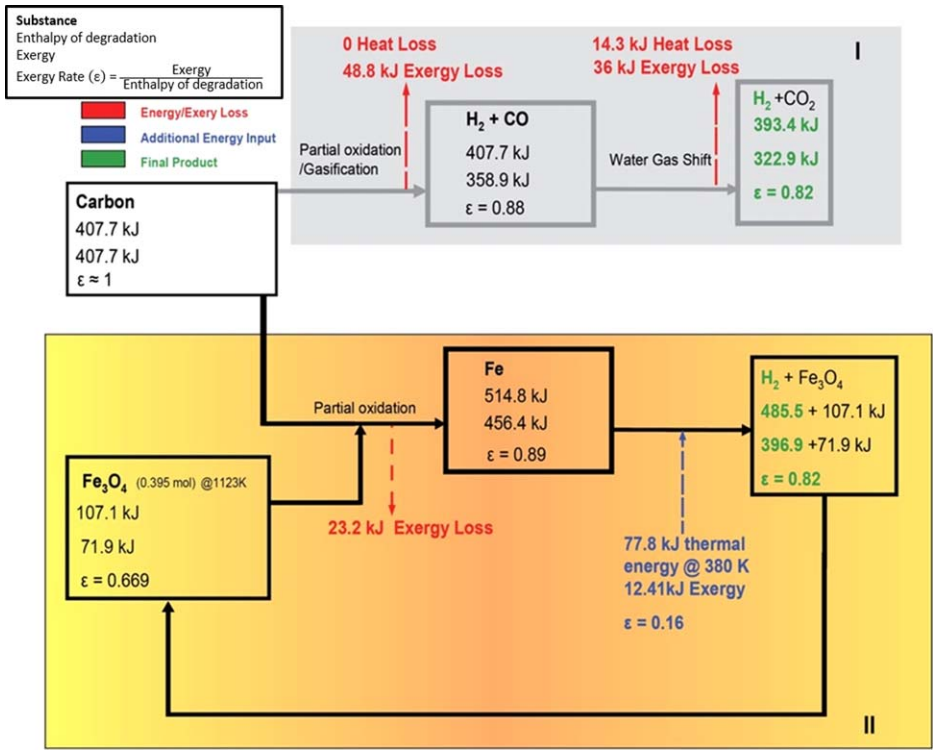

Figure 4. Exergy recovery analysis for two H_2 production schemes with a reaction temperature in II of 1123 K.

Fe_3O_4 in a high-temperature solar reactor, were also initiated.[28] It was found that although the fluidized particles were effective in absorbing solar radiation, the high cost of the solar energy conversion, the sintering and recrystallization of metallic iron, and the low methane conversion contributed to the slow development of this solar-based chemical-looping process. Metal oxide redox pairs, such as ZnO-Zn and Fe_3O_4-FeO/Fe, were used for type B-III water-splitting solar thermochemical cycles.[29,30] Recently, more elaborate materials such as $Co_{0.85}Fe_{2.15}O_4$ and Fe_2O_3 composite thin films supported on ZrO_2 synthesized with atomic layer deposition indicated encouraging activities for isothermal water-splitting reactions in solar-based redox cycles.[31]

Since the early 2000s, several pilot-scale units of chemical-looping processes have been constructed for renewed large-scale demonstrations of the technology. Notably, a 1-MWth chemical-looping combustion process is being demonstrated at the Technical University of Darmstadt in Germany with ilmenite as the oxygen carrier and with coal as the feedstock. The reactors for both the reducer and the combustor are circulating fluidized beds.[32] The high-pressure pilot syngas chemical-looping (SCL) process of OSU is being demonstrated at the National Carbon Capture Center (NCCC) at 250 kWth to 3MWth to produce hydrogen with syngas derived from coal gasification or natural gas as the feed.[33] The reducer and oxidizer are moving-bed reactors, whereas the combustor is a fluidized bed. Two pilot plants are being developed for calcium-looping operations to capture CO_2 from a flue gas stream. One is a 1.7-MWth demonstration pilot plant in Spain operated by a consortium led by the mining company HUNOSA.[34] Both the calcination and carbonation reactors are a circulating fluidized bed. The other is a 2-MWth plant in Taiwan, operated by Industrial Technology Research Institute (ITRI), and is conducted with both the calcination-carbonation and calcination-carbonation-hydration schemes.[35] This is a demonstration of OSU's calcination and carbonation reaction (CCR) process technology.[36] ITRI's CO_2 capture operation is linked to a cement production plant nearby. Furthermore, the installation at the Technical University of Darmstadt used for chemical-looping combustion is also being used for operation in the calcium-looping mode with one of the circulating fluidized-bed reactors performing carbonation, whereas the other circulating fluidized bed performs calcination in a manner similar to the pilot unit in Spain.[37]

Motivation in Modern Chemical-Looping Process Development

The modern chemical-looping approach is motivated by two factors: (1) the pressing need to mitigate climate change because of CO_2 emissions with efficient and cost-/energy-effective CO_2 capture from methods in the combustion of fossil fuels[38–41] and (2) the optimization of reaction schemes to minimize the exergy loss involved in the chemical/energy conversion system.[5,6,42,43]

CO_2 capture

Current coal combustion power plants require equipment for the removal of such environmentally hazardous air pollutants such as sulfur oxides, nitrogen oxides, fine particulates, and mercury in the flue gas, and the installation of additional

equipment for the capture of CO_2 may be required in the future. The total amount of CO_2 produced from coal-based power plants accounts for more than 40% of all anthropogenic CO_2 emissions.[44] CO_2 management involves three steps: (1) capture, including separation and compression; (2) transportation; and (3) sequestration. Among the three steps, CO_2 capture is the most energy-consuming one.[45] CO_2 represents about 15% of the flue gas stream from coal combustion power plants, and the existing techniques for CO_2 capture from pulverized coal power plants include the well-established monoethanolamine scrubbing technology and the chilled ammonia process.[46]

Similar to solvent-based CO_2 scrubbing techniques, high-temperature sorbents, such as limestone, potassium carbonates, lithium silicates, and sodium carbonates, can be used to capture CO_2 in the flue gas at elevated temperatures.[47,48] With good heat integration, these solid sorbents can be effective in CO_2 capture. One heat integration scheme is of particular relevance and is based on the type A-II chemical looping that uses hydrated lime, natural limestone, or re-engineered limestone based sorbents at 600–700°C for CO_2 capture.[49] In the process, both CO_2 and SO_2 in the flue gas are captured by the calcium-based sorbents in the carbonator operated at about 650°C to form $CaCO_3$ and $CaSO_3/CaSO_4$. The carbonated sorbent, $CaCO_3$, is then regenerated to a calcium oxide (CaO) sorbent in the calciner at 850–900°C to yield a pure CO_2 stream. In type A-I chemical looping, discussed earlier, the oxygen carrier is reduced by the fuel in the first reactor (reducer or fuel reactor) and produces CO_2 and H_2O. The reduced oxygen carriers are then transported to the second reactor (oxidizer, combustor, or air reactor) where combustion takes place with air and the reduced oxygen carrier is converted to its original oxidation state. During the oxidation step, a large amount of heat is generated, which can be used for electricity generation. Because air and fuels are converted in separate reactors, the CO_2 generated from the reducer is only mixed with steam and is readily separable. The capital- and energy-intensive conventional CO_2 separation step can be avoided.

Exergy loss minimization

The indirect fuel conversion in two separate reactors is advantageous from a thermodynamic point of view for the reduction of exergy loss. The exergy of a system is defined as the maximum amount of usable work from the system during a transformation that brings the system into equilibrium with a reference state.[50] The ambient environment (at 273.15 K and 101.325 Pa) is commonly used as the reference state. The reference states for some chemical species include: 400-ppm CO_2 in the air for CO and C; H_2O for H_2; and Fe_2O_3 for Fe, FeO, and Fe_3O_4. The exergy rate refers to the ratio of the exergy to the enthalpy of the system. The loss of exergy in a system implies the loss of utilizable energy and can be mitigated by two approaches. The first approach is done through thermomechanical means by recuperation of the discharged low-grade heat and/or by the generation of a larger amount of high-grade heat. The second approach is through the use of the chemical intermediates that recuperate heat in a circulatory reaction system. The second approach is of close relevance to the chemical-looping processes.[4,51] As an example, Figure 4 shows two schemes converting char (assumed to be pure carbon) to hydrogen with steam. Scheme I in this figure represents a traditional hydrogen production route where carbon is gasified and coupled with the WGS reaction. With the reference states given previously, the exergy calculations for various streams are shown in Figure 4. With the conventional route, a 48.8-kJ exergy loss in the gasification/partial oxidation step is seen. The WGS reaction leads to another 36-kJ exergy loss. An alternative approach with the Fe-Fe_3O_4 chemical-looping method is considered in Scheme II in Figure 4 and consists of the following reactions:

$$C+0.395Fe_3O_4+0.21O_2 \rightarrow 1.185Fe+CO_2 \quad (1)$$

$$3Fe+4H_2O \rightarrow Fe_3O_4+4H_2 \quad (2)$$

A small amount of O_2 is used in the first reaction to neutralize the heat of the reaction. Because of the generation of

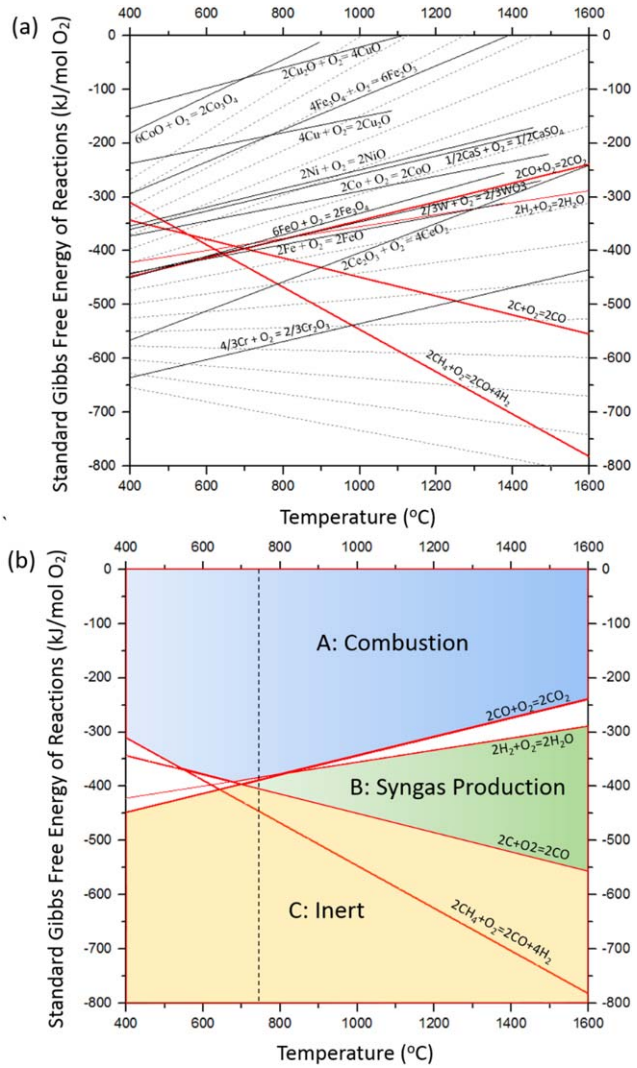

Figure 5. Modified Ellingham diagram for oxygen-carrier materials: (a) Standard Gibbs free energy changes (ΔG_r^o) of some oxidation reactions and (b) reaction zone division for chemical-looping combustion and syngas production applications.

Fe (a medium-exergy-rate chemical) from Fe_3O_4 (a low-exergy-rate chemical), a 52.4% lower exergy loss occurs in step 1 (23.2 kJ) as compared to the exergy loss in a traditional gasification step (48.8 kJ). The steam-iron reaction in step 2 of Scheme II in Figure 4 only needs a minimal amount of low-grade heat, and zero exergy loss is achievable in this step of the scheme. As a result, the net exergy loss for H_2 production is reduced by 27%. The details of the exergy calculation for this example and the other chemical-looping processes and their impact on the process-intensification strategy for the reduction of capital and operating costs are available in the literature.[4,8] The reduction of exergy loss with a chemical-looping scheme can result in a thermal power plant efficiency as high as 50% (lower heating value, LHV).[1]

Although extensive research is ongoing globally to substantiate the commercial potential of chemical-looping processes, for successful application of this technology, considerable attention has been given to two key aspects: one is concerned with the oxygen carriers,[52,53] and the other is concerned with the reactor configurations.[4,8]

Oxygen Carriers

In the reduction reaction for types A-I and B chemical-looping systems, the lattice oxygen in the metal oxygen carrier is transferred to the fuel to perform full and partial oxidation, respectively. The selection of the oxygen-carrier materials and its synthesis method require a thorough knowledge of the properties and intended applications of the oxygen carrier, including the equilibrium phase behavior of the metal oxides, kinetics of the redox reactions, temperature and pressure effects, mechanical properties such as attrition, recyclability, heat-transfer properties, process configurations, reaction products, and potential formation of undesired products, such as from carbon deposition. Furthermore, for chemical-looping processes to be commercially viable, the materials and synthesis costs for the oxygen carriers must be low.

Thermodynamic analysis

The selection of metal oxides can be made on the basis of a modified Ellingham diagram, as shown in Figure 5,[54] where the standard Gibbs free energy change variations with the temperature is given according to the following reaction:

$$a\mathrm{Me}_x\mathrm{O}_y + \mathrm{O}_2 = a\mathrm{Me}_x\mathrm{O}_{(y+2/a)} \quad (3)$$

This is in contrast to the original Ellingham diagram, in which the standard Gibbs free energies of the formation of metal oxides are used. Note that in the modified Ellingham diagram, the reduction-oxidation pair that coexists at equilibrium in eq. 3 are represented by a pair of a metal and its adjacent metal oxide or a metal oxide and its adjacent metal oxide at a higher oxidation state, as defined in the phase diagram of the metal oxides. On the basis of the modified Ellingham diagram, metal oxide materials can be grouped into several zones, depending on their applications, as shown in Figure 5(b).[54] The zones in the figure are bound by three key lines represented by the following reactions:

$$\text{Reaction line 1: } 2\mathrm{CO} + \mathrm{O}_2 = 2\mathrm{CO}_2 \quad (4)$$

$$\text{Reaction line 2: } 2\mathrm{H}_2 + \mathrm{O}_2 = 2\mathrm{H}_2\mathrm{O} \quad (5)$$

$$\text{Reaction line 3: } 2\mathrm{C} + \mathrm{O}_2 = 2\mathrm{CO} \quad (6)$$

Specifically, the materials in zone A given in Figure 5(b) have strong oxidizing properties and can work as oxygen carriers for both full oxidation and partial oxidation. The molar ratio of the lattice oxygen in the oxygen carrier to the fuel in the feed determines whether the reaction is either partial or full oxidation. For a given feedstock flow rate, less oxygen is required for partial oxidation than for full oxidation. For the materials in zone B, the reaction proceeds in partial oxidation, and an excessive amount of oxygen carrier does not yield full oxidation. Metal oxides in zone C cannot be used as oxygen carriers and are considered inert materials. Although the modified Ellingham diagram was developed for single metal oxides, a similar diagram for complex metal oxides can be developed and likewise applied. It should be noted that the modified Ellingham diagram only provides the thermodynamic properties for metal oxide materials. Other properties, such as reaction kinetics, also need to be considered in the metal oxide selection.

Single and supported metal materials

Pure active metal oxide oxygen carriers deteriorate in their performance over multiple reduction-oxidation reaction cycles.[55,56] Single metal materials, such as $CaSO_4$, with a low cost and a high oxygen-carrying capacity have been extensively studied. However, the reduction reaction of $CaSO_4$ to CaS leads to sulfur leakage (in SO_2 form) and CaO formation; this leads to decreased $CaSO_4$ reactivity and recycability.[57] Metal oxide oxygen carriers have a tendency to sinter during high-temperature reactions, and this results in reductions in the surface area and pore volume. Macroscopically, the oxidized gaseous products formed during the reduction of the oxygen carriers move from the solid surface to the bulk gas phase, whereas during the oxidation of the reduced oxygen carriers, the reaction can occur on the surface or in the inner part of the carriers. The reduction and oxidation of pure active metal oxide oxygen carriers yield volume contraction and expansion, respectively, accompanied by the formation of micropores. Micropores formed during the reactions facilitate reactive gas diffusion inside the particle. At the grain level, reduction and oxidation reactions occur via ionic diffusion.[58] The ionic diffusion can take place in three modes: (1) outward diffusion mode, (2) inward diffusion mode, and (3) mixed diffusion mode. Most reactions follow the mixed diffusion mode, where either the inward diffusion mode or the outward diffusion mode dominates. During the formation of the wüstite and magnetite phases from pure Fe, the outward diffusion of iron cations is the dominant diffusion mode, whereas in the formation of the hematite phase, the inward diffusion of oxygen anions is the dominant mode.[59] The diffusion mode can be altered by the addition of a support material.[60–62] The addition of TiO_2 to iron oxide facilitates the diffusion of oxygen anions; this results in superior reactivity over multiple redox cycles.[58] It is noted that the oxygen ion diffusion energy barrier is significantly lower in $FeTiO_3$ compared to that in FeO. This low energy barrier results in faster reaction kinetics of ilmenite as compared to that of FeO; ilmenite ores are

regarded as naturally occurring TiO_2-supported iron oxide oxygen-carrier materials.[58,63,64]

The morphological changes of iron oxide materials during the redox reactions can be examined more closely at the nanoscale or microscale for their effects on the reactivity and recyclability in the chemical-looping systems. Figure 6 shows the scanning electron microscope (SEM) image and energy-dispersive X-ray spectroscopy (EDS) mapping of the iron oxide microparticles. The ionic diffusion of pure Fe during oxidation creates a porous center, shown in Figure 6(a), as opposed to the random pore distribution initially seen, as given in Figure 6(b). During Fe oxidation, about a 25% volume expansion also occurs.[65] As shown in Figure 6(c,d), during Fe oxidation, two types of nanostructures, nanowires, and nanopores, are developed on the particle surface.[65] The formations of these structures are due to a stress-driven mass transport, caused by volume expansion during oxidation.[66] These nanostructure formations are heavily dependent on the positive or negative grain/crystallite surface curvature. They disappear when oxidation is followed by reduction, which occurs via outward diffusion of oxygen ions, and leads to the formation of vacancies. The aggregation of vacancies creates micropores throughout the particle volume and causes the disappearance of these nanostructures. The voids created inside the materials during the first oxidation-reduction cycle lower the surface stress during the subsequent cycles. Hence, these nanostructures are only observed during the first cycle. Fe materials, having undergone multiple redox cycles, often form irreversible agglomerates because of sintering effects. This effect causes the pure Fe to be deactivated over time during redox chemical-looping processes. In the case of a binary system, such as an Fe-Ti alloy, increasing the number of redox cycles increases the porosity of the alloy microparticle, as shown in Figure 7.

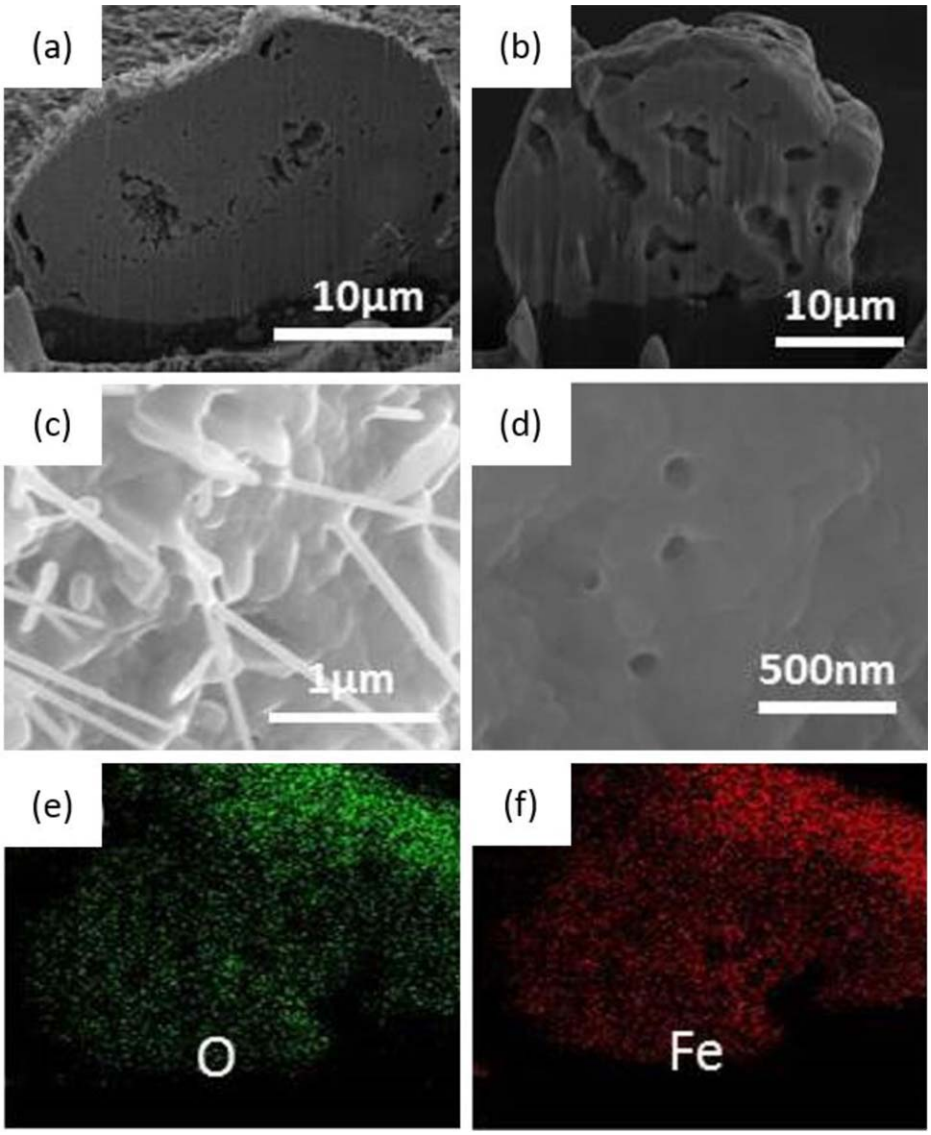

Figure 6. Characterization of the iron oxide microparticles: (a) SEM image of the cross section of Fe_2O_3 particles after Fe oxidation, (b) SEM image of the cross section of fresh Fe particles, (c,d) SEM images of nanowires and nanopores on the top surface of the Fe_2O_3 particles, (e) EDS mapping of O from part a, and (f) EDS mapping of Fe from part a.

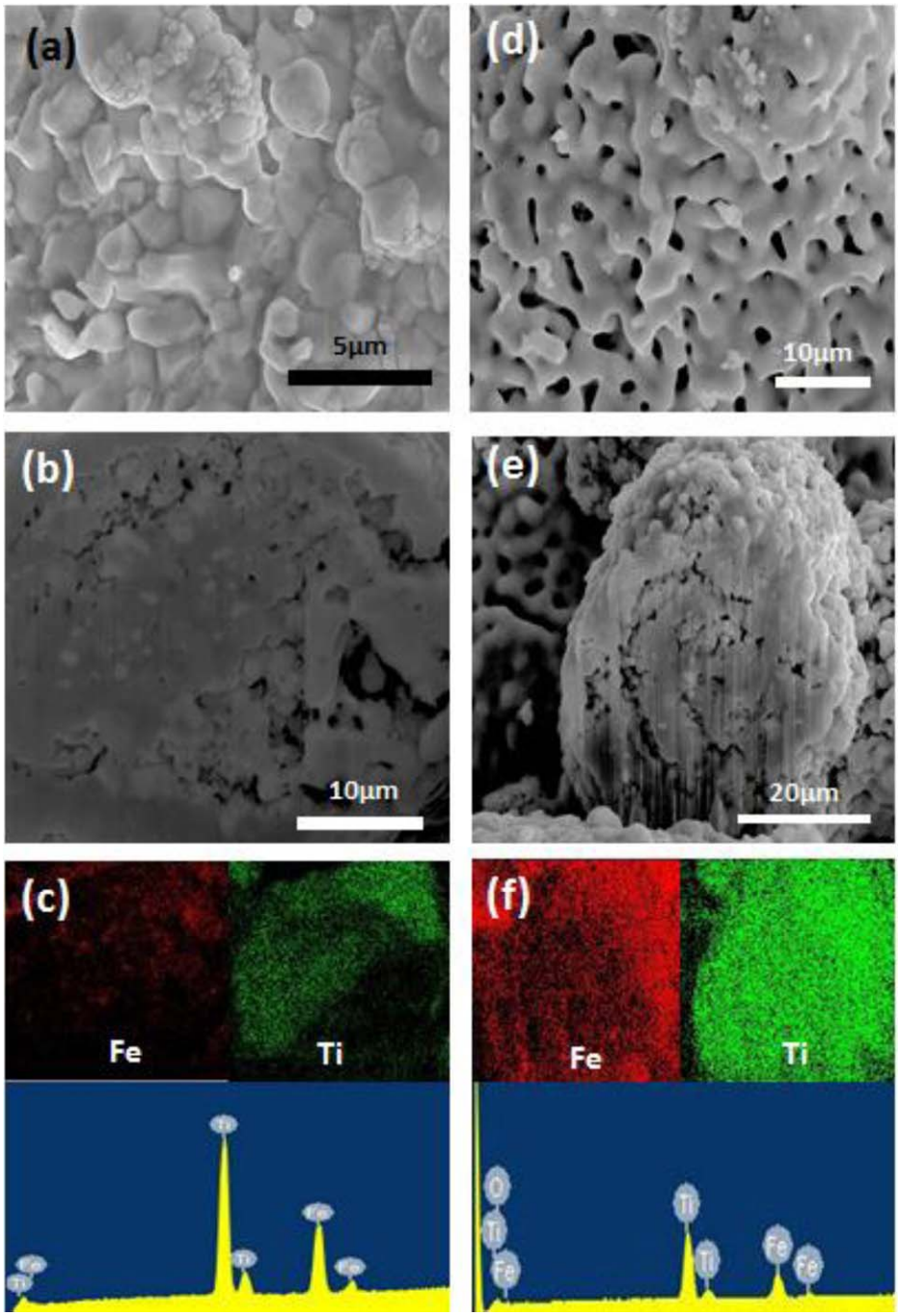

Figure 7. (a-c) Characterization of the Fe-Ti microparticles after one oxidation-reduction cycle. (a) SEM image of surface. (b) SEM image of the cross section. (c) EDS mapping and spectrum of the surface. (d-f) Characterization of the Fe-Ti particles after five oxidation-reduction cycles. (d) SEM image of the surface. (e) SEM image of the cross section. (f) EDS mapping and spectrum of the surface.

Ti acts as a support material to the active Fe phases. The addition of Ti assists in reducing the sintering effect and enhancing the porosity and lattice vacancies that promotes pore diffusion and ionic diffusion. Hence, a binary system of Fe and Ti can undergo multiple redox cycles and still maintain its reactivity. Under high-pressure oxidation-reduction cycles, high-particle porosity within the metal oxides is observed. These porosity effects corroborate the faster redox kinetics observed at higher pressures as compared to atmospheric pressures.[67]

The effects of the addition of support materials on the ionic diffusion behavior and the morphology during redox reactions can be further elaborated with two well-mixed supported oxygen-carrier systems: Fe_2O_3/TiO_2 and Fe_2O_3/Al_2O_3. In these systems, Fe_2O_3 is the active metal oxide, whereas TiO_2 and Al_2O_3 are used as support materials. Each of them is subjected to 50 consecutive redox cycles. At the end of 50 cyclic reduction-oxidation reactions, a core-shell structure is formed in the Fe_2O_3/Al_2O_3 system. In the Fe_2O_3/TiO_2

system, the well-mixed condition of the metal oxides remains. In the Fe_2O_3/Al_2O_3 system, the redox reactions proceed with the diffusion of iron cations from the particle interior to the particle surface to form an Fe_2O_3 shell with Al_2O_3 in the core.[68] On the other hand, in the Fe_2O_3/TiO_2 system, the redox reactions proceed with the diffusion of oxygen anions; the active phase expands and shrink locally; this maintains the well-mixed form of the Fe_2O_3/TiO_2 particles. For chemical-looping processes, oxygen carriers that continue to be highly reactive over a long term of reactions are desirable. The formation of the core-shell structure manifests a phase separation that is undesirable for the recyclability of metal oxide carriers. Generally, the metal oxide oxygen carriers with support materials can minimize the volume contraction and expansion of the carriers upon reduction and oxidation; hence, it is easy to maintain the integrity of solid materials during the reactions.

Active binary systems or mixed metal oxide based oxygen carriers have garnered considerable interest recently. Ferrites [$M_xFe_{3-x}O_4$ (M = Ni, Co, Zn, or Cu, $0 < x < 1.5$)] are becoming a particularly popular choice for oxygen carriers. Most ferrites have a spinel structure. $NiFe_2O_4$, synthesized from Fe_2O_3 and NiO by ball milling and high-temperature calcination, exhibited improved reactivity and recyclability for hydrogen production from the steam iron reaction.[69] $NiFe_2O_4$ has also been tested as an oxygen carrier and catalyst for the partial oxidation of methane to syngas. Because nickel is known to be an effective catalyst for steam methane reforming (SMR), the idea of using mixed metal oxides as oxygen carriers in the first stage and the generated metallic nickel as a catalyst for the second stage of SMR is of practical interest. The redox reactions of Fe-Ni systems involve complex morphological variations because of the ionic diffusion and volume expansion phenomena. Oxidation of a binary Fe-Ni system is represented by an Fe_2O_3-rich shell and an NiO-rich core formation with the volume expansion upon oxidation during the first redox cycle.[65,70] This is a result of Ni having a faster oxidation rate and smaller volume expansion rate than Fe during oxidation. Ni ions react with oxygen first and remain in the core, whereas Fe ions tend to diffuse out of the core; this is driven by the ionic concentration gradient of Fe and the high volume expansion rate of Fe to Fe_2O_3. However, the core-shell structure disappears with uniform Fe and Ni distribution in the particles after multiple redox cycles.

CLOU and perovskites

In certain oxygen carriers, molecular oxygen can be released in sufficient concentrations, and this can provide effective oxidation reactions for the fuels. Metal oxides that possess this property are noted as CLOU materials. A high reaction rate for the oxidation reaction of the fuel is an advantage of these CLOU materials.[71,72] Typical CLOU materials include CuO, Co_3O_4, and Mn_2O_3; they have disadvantages in terms of their melting point, environmental health, and oxygen-carrying capacity, respectively. In recent years, binary CLOU and metal oxide materials have been studied.[73,74] For example, copper ferrites ($Cu_xFe_{3-x}O_4$, with $0.3 < x < 1.5$) were tested for methane partial oxidation. They had a lower CH_4 conversion and selectivity compared to iron oxides and showed no carbon deposition. The reduced phases consisted of Cu, Cu_2O, $CuFeO_2$, and/or Fe_3O_4, depending on the reaction conditions. For these materials, the phase migration, together with the formation of Cu_2S and $FeSO_4$ during the reaction with high-sulfur-content fuel, may lead to irreversible structural changes and may deteriorate the recyclability.

As indicated, variations in the ionic diffusivity and morphological properties play important roles in determining the recyclability of the oxygen carriers during the reduction-oxidation cycles. Knowing that the structure of the perovskite materials can provide excellent electron and ionic conductivities, considerable studies have been devoted to the use of perovskite materials, either alone or in combination with other active metal oxides or support for use as oxygen carriers. Perovskite materials have a general formula of ABO_3 and are characterized by nonstoichiometric oxygen with a high oxygen diffusivity.[75–79] For example, $CaMnO_{3-\delta}$, which can be synthesized from calcium oxides and manganese oxides, was found to have a desirable reactivity, strong mechanical strength, and high melting point. However, the perovskite structure of $CaMnO_{3-\delta}$ is not stable and tends to decompose to $CaMn_2O_4$ and $Ca_2MnO_{4-\delta}$ in a reducing environment. To improve its performance, several types of transition metals, including Fe, Ti, Mg, Cu, and La, were used as partial substitution of Mn atoms.[80,81] The substitution of a part of Mn with Ti has indicated improved oxygen-carrier performance. It was found that the substituting metal ions needed to be of a similar size as Mn; otherwise, the segregation of metal ions could take place in the particle. Thus, Mg was found to be an undesirable candidate as a substituting atom for the B site.

In addition to the type of $CaMnO_{3-\delta}$ perovskite materials, the type of $AFeO_3$ (A = La, Nd, and Eu) perovskite materials has also been synthesized and tested.[82] Two stages of the reaction process were observed during the reaction of $AFeO_3$ with methane. A significant amount of CO_2 was formed in the first stage, although a high-purity syngas was generated in the second stage. Among these three perovskite materials, the highest yield of syngas was obtained with $LaFeO_3$ as the oxygen carrier. With the addition of a small amount of other components, the performance could be further improved. More metals could be included in the substitution for perovskite materials as in $La_{1-x}Sr_xM_yFe_{1-y}O_3$ (M = Ni, Co, Cr, or Cu).[83] Complex metal oxides materials have also been used for chemical-looping reactions with specific applications to hydrogen generation.[84] The fundamental nature concerning the interplay of various metal ions for complex materials is more difficult to probe aside from the complexity involved in the synthesis and the cost associated with their practical use.

Reactor Configurations

The reducer and combustor are two key reactors in chemical-looping systems. Considering type A-I and type B-I chemical-looping systems with iron-based metal oxides as oxygen carriers, the combustor is uniquely suited with a fluidized bed or a riser because of its good mass and heat transfer properties. The reactions in the combustor are intrinsically fast and thermodynamically favored. In contrast,

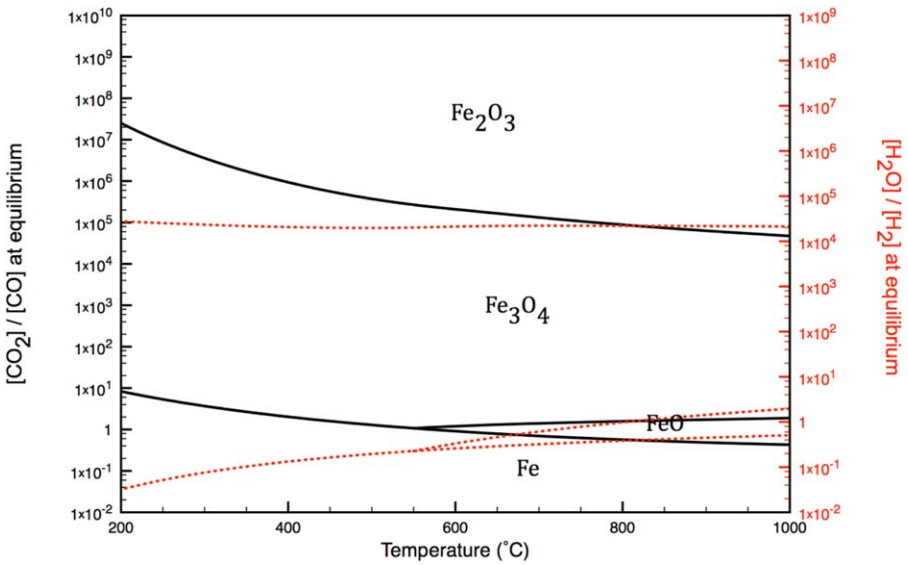

Figure 8. Equilibrium phase diagram for the $Fe/FeO/Fe_3O_4/Fe_2O_3$ system for redox reactions with CO_2/CO (solid lines) and H_2O/H_2 (dashed lines).

the reduction reactions are relatively slow and thermodynamically limited. An optimum design of a reducer with a thermodynamically favored gas-solid contacting pattern is thus desired. The design of chemical-looping reducers under continuous solids flow conditions can mainly be classified on the basis of the contacting patterns of the fuels and oxygen carriers, including mixed contact, cocurrent contact, and countercurrent contact. The flow pattern in the mixed contact can be represented by a single fluidized bed, whereas that in the cocurrent contact and countercurrent contact can be represented by a moving bed or a series of fluidized beds. It is noted that fixed beds under solid batch conditions can also be used with gaseous feedstock for the reducer and combustor operations.[85–88] However, it can be used only when the gas flow control at high temperatures can be properly implemented at the feedstock feeding point and product discharging point of the reactors. Depending on the type of the reactor used, the oxygen-carrier particle size can vary from 50 μm to 5 mm.

Small-scale systems for chemical-looping combustion have been extensively studied including the french institute of petroleum (IFP) 10-kWth chemical-looping combustion (CLC) system (France); the Chalmers University of Technology 10- and 100-kWth CLC system (Sweden); the Instituto de Carboquimica 1.5-, 10-, and 50-kWth CLC system (Spain); the Vienna University of Technology 120-kWth CLC system (Austria); the Korea Institute of Energy Research 50-kWth CLC system (Korea); the Southeast University 1-, 10-, and 50-kWth solid-fuel CLC system (China); the Western Kentucky 10-kWth CLC system (US); and the University of Utah 100-kWth CLC system (US).[89–101] Among these studies, the feedstock of primary interest has been solid fuels, such as coal and gaseous fuels, such as syngas and natural gas. Challenging factors in the design of a reducer for a solid-fuel chemical-looping system include the kinetics of the solid-fuel gasification and the solid-fuel residence time. In fluidized-bed reducers, the fluidizing gas is usually CO_2 and/or steam; this also serves as an enhancing gas to promote solid-fuel gasification kinetics. To increase the residence time of a solid fuel, the contact pattern in fluidized-bed reducers can be altered. For example, a spouted bed can be used to provide a longer residence time for solid-fuel reactions.[97–99] In some systems, a carbon stripper has been added between the reducer and oxidizer to separate and recycle unconverted char discharged from the reducer.[92,93] However, this is a remedial step in overcoming the char discharge to the combustor directly from the fluidized bed and, thereby, enhances the carbon-capture efficiency. This step also assists in the separation of ash from the oxygen carrier before the combustor is entered. The channeling behavior of the fluidized bed also provides a direct path for leakage of the volatiles from the reducer; this then requires a separate volatile treatment device outside the reducer.

The oxygen-carrier conversion with a fluidized-bed reducer is constrained by thermodynamic limitations. To illustrate, consider the conversion of iron oxide in a fluidized-bed reducer and a countercurrent moving-bed reducer for CO combustion. The comparisons can be made through the examination of the phase diagram of iron oxide in the presence of CO and CO_2, as shown in Figure 8. In a well-mixed fluidized-bed reducer, the gas inside the bed and in the bed outlet is rich in CO_2, and thus, the Fe_2O_3 cannot be sufficiently reduced as reflected by the iron oxide phase diagram. As an example, to achieve a 99.99% CO conversion from the fluidized-bed reducer, the Fe_2O_3 cannot be reduced to an oxidation state lower than Fe_3O_4; this corresponds to a solid conversion of no more than 11.1%. In contrast, in a moving-bed reducer with a countercurrent gas-solid contacting pattern, Fe_2O_3 can exit the reducer with an oxidation state lower than Fe_3O_4 with a fresh CO feed countercurrently flowing to it. Under the countercurrent moving-bed operating conditions, more than 99.99% of CO can be converted, and the solids can be reduced to an FeO/Fe mixture. This correspond to a solid conversion of around 50%.[102] The same principle can be applied to the processing of other gaseous feedstocks, including H_2, CH_4, and coal/

biomass volatiles. For a given fuel input, the Fe_2O_3 circulation rate in a countercurrent moving-bed reducer is less than 25% that of a fluidized-bed reducer. The ash separation can be readily achieved inside the solid-fuel moving-bed reducer because of the particle size difference between the oxygen carrier and ash. This further reflects the advantage of the countercurrent moving-bed operation for type A-I applications.[4]

For type B-I applications for syngas production, a well-mixed fluidized-bed reducer possesses a wide residence time distribution range; this yields a mixture of oxygen carriers in various states of reduction. For iron-based oxygen carriers, high oxidation states produce a syngas of low purity, whereas low oxidation states produce a syngas of high purity. However, the low oxidation states of iron-based oxygen carriers tend to catalyze the carbon deposition reactions. Gas channeling in a fluidized bed can produce a gas mixture consisting of unreacted fuel and syngas at the reactor outlet. Alternatively, in a moving-bed reactor with a cocurrent gas-solid flow pattern, the residence time distribution and the extent of the oxygen-carrier conversion can be accurately controlled while preventing carbon deposition.[67,103] At the inlet of the reactor, the high concentration of fuel feed reacts with the high-oxidation-state metal oxides. At the reducer outlet, carbon deposition can be prevented or minimized because of the low concentration of unreacted fuel. When the reduced oxygen carriers consist of a redox pair in zone B, as shown in Figure 5, full oxidation of the fuel can be prevented, and syngas can be generated. Thus, significantly improved gas and solid conversions over the fluidized bed can also be achieved when a cocurrent moving bed is used as the reducer for gasification applications.

OSU Chemical-Looping Technologies

OSU has actively engaged in chemical-looping technology development since the mid-1990s. The chemical-looping technologies developed at OSU are continually evolving in scale and range from bench scale to pilot scale. One central feature of OSU technologies for types A-I and B-I is the use of a moving-bed reducer reactor. OSU technologies are capable of converting carbonaceous feedstocks, including coal, natural gas, liquid hydrocarbons, biomass, petroleum coke, and char, into products such as heat, electricity, syngas, hydrogen, and chemicals with inherent CO_2 capture. Five OSU chemical-looping technologies have been developed and demonstrated at the subpilot or pilot-scale operation: the calcium-looping process (CLP), the CCR process, the SCL process, the coal-direct chemical-looping (CDCL) process, and the shale-gas-to-syngas (STS) process. The coal-to-syngas (CTS) process has been demonstrated at the bench scale.

CLP: type A-II

The CLP produces hydrogen (H_2) while simultaneously removing CO_2 in the WGS reaction using a calcium-based sorbent. Calcium hydroxide [$Ca(OH)_2$] is used to overcome the equilibrium limitation of the WGS reaction. In addition to CO_2 removal through the formation calcium carbonate ($CaCO_3$), the process also removes sulfur ($H_2S + COS$) and halide (HCl/HBr) impurities to form, calcium sulfide (CaS), and calcium halide (CaX). The process parameters can be adjusted to produce a syngas suitable for fuel/chemical synthesis by the Fischer-Tropsch reaction. The $CaCO_3$ formed in the WGS reactor is then calcined to regenerate CaO and produce a sequestration-ready CO_2 stream.[104] Such regeneration, however, requires the calcination temperature to be above 900°C; this results in the significant sintering of CaO. The sintered CaO is then reactivated by hydration to form $Ca(OH)_2$. This constitutes the basic three-step CLP for H_2 production.

The process concept has been verified on a laboratory-scale fixed-bed reactor and on a subpilot scale entrained-bed reactor for the integrated WGS reaction, and CO_2 capture, and sulfur and halide removal.[36] The continuous flow of $Ca(OH)_2$ and simulated syngas has been tested at the subpilot scale, which has a residence time on the order of seconds. The isothermal, subpilot-scale experiments conducted at 600°C in the absence of any WGS catalyst at atmospheric pressure resulted in about a 70% H_2 product purity (on a steam-free basis) and the complete removal of CO_2 generated from WGS. The $Ca(OH)_2$ also holds an advantage over conventional CaO sorbents, in that it aids the WGS reaction by providing an additional source of steam upon decomposition at the reaction temperature. At high pressures (ca. 21 atm), fixed-bed results have obtained a high CO conversion with more than 99% H_2 purity at near stoichiometric steam-to-carbon ratios.[105]

The CLP technology has been evaluated for techno-economic feasibility by comparison with US Department of Energy (DOE) baseline reports for an oxygen-blown coal-to-hydrogen plant and methane-to-hydrogen plant with SMR.[106–108] The process simulation results for the CLP technology were derived with the same assumptions as were used for the corresponding baseline cases.[109–111] The baseline first-year cost of H_2 from coal and with a conventional CO_2 capture technology is \$3.15/kg.[107] The corresponding first-year cost of H_2 from coal with CLP technology is \$2.77/kg H_2.[106] The SMR case with CLP technology gives the first-year cost of H_2 as \$ 1.99/kg H_2.[106] This is a significant improvement over the \$ 2.20/kg H_2 cost reported in the baseline case with SMR technology. Overall, the CLP technology reduces the cost of hydrogen production by 10–12% when compared to the conventional CO_2 capture and WGS technologies.

CCR: type A-II

The carbonation calcination reaction process is for post-combustion carbon dioxide control.[8,36] The CCR process uses a solid sorbent in a three-reactor loop to simultaneously remove both CO_2 and SO_2 from postcombustion flue gas streams whereas also producing additional electricity. The solid sorbent source is limestone or calcium carbonate ($CaCO_3$). In the CCR process, $CaCO_3$ is first decomposed into calcium oxide (CaO) and CO_2 in a calciner in a similar manner as that in the CLP. This decomposition reaction is endothermic and requires oxycombustion to generate a sequestration-ready stream of CO_2. An intermediate high-temperature hydrator is then used to convert CaO to $Ca(OH)_2$; it operates at temperatures between 300 and 500°C. The resulting solid $Ca(OH)_2$ is used to remove CO_2

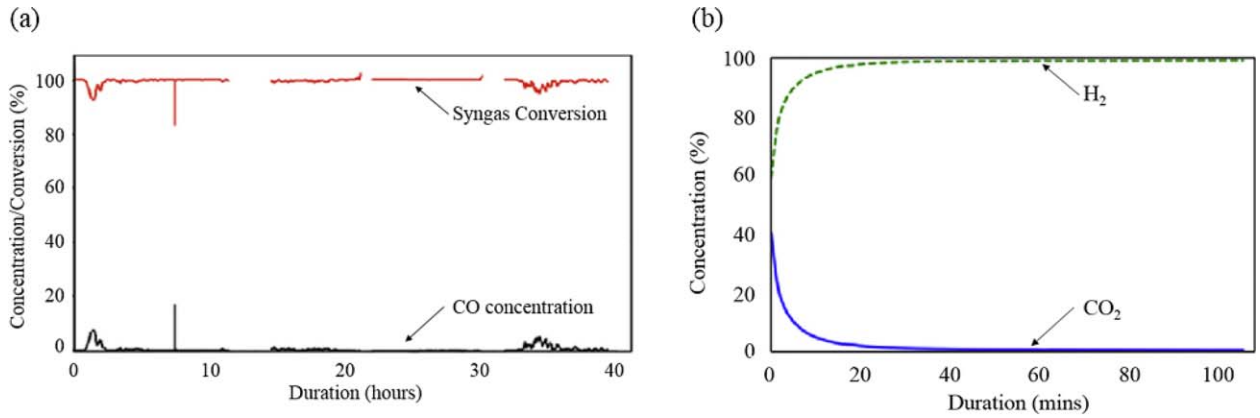

Figure 9. OSU SCL subpilot plant for hydrogen generation and CO_2 capture: (a) syngas conversion and carbon monoxide concentration at the reducer gas outlet and (b) hydrogen and carbon dioxide concentrations at the oxidizer gas outlet.

and SO_2 from a flue gas stream. In the carbonator, the $Ca(OH)_2$ reacts with CO_2 to form $CaCO_3$ and SO_2 to form calcium sulfate ($CaSO_4$). The solid loop is then complete. The formed $CaSO_4$ is inert in the CCR process and, if not removed through a purge stream, will accumulate over multiple cycles. The purge stream reduces the circulation of inerts, such as $CaSO_4$, ash, and limestone impurities.

The CCR process has been conducted at the 120-kWth scale with a mixture of coal and natural gas to produce the flue gas.[36] The carbonator was an entrained-bed reactor. The single-cycle experiments were used to obtain the relationship between the calcium-to-carbon (Ca/C) molar ratio and extent of CO_2 and SO_2 removal. A 90% CO_2 removal was achieved at a Ca/C molar ratio of 1.3 with calcium hydroxide. Over multiple cycles, no reduction in the CO_2 removal performance was observed. As noted earlier, the CCR process was demonstrated by ITRI at the 2-MWth scale.[35] ASPEN PLUS process simulations on the high-temperature CCR process have been reported.[8,36] The base power plant results follow case 11 of the DOE baseline report.[108] The CCR process was modeled on the basis of DOE energy system analysis guidelines.[109–111] The CCR process requires 150 MWe of auxiliary power, mainly for CO_2 compression and air separation, but an additional 500 MWth of high-quality heat is generated by the CCR process, and thereby, the energy penalty for the CCR process is minimal.

SCL type A-I process

The SCL process converts gaseous fuels such as syngas and natural gas by the high-temperature cyclic reduction and oxidation of iron oxide based oxygen carriers.[102,112,113] The process can be designed to cogenerate heat and hydrogen while producing a sequestration-ready CO_2 stream. Clean syngas from a conventional gasifier is introduced into a countercurrent moving-bed reducer. In the reducer, the syngas is converted to steam and CO_2, and the oxygen carriers are reduced. The reduced oxygen carriers are first partially oxidized with steam in the oxidizer, thereby producing hydrogen, and then, it is completely reoxidized with air in the combustor. The oxidation reactions are highly exothermic, and the heat generated is partially used to generate electricity via steam turbines. Thus, CO_2, H_2, and heat are generated in three separate reactors; this obviates the need for any downstream product separation.

A comprehensive analysis at OSU established that iron oxide is an ideal choice for an oxygen carrier, both from the process performance and economic standpoints.[33] The reactors in the SCL process are designed based on comprehensive thermodynamic analysis and kinetic modeling,[102,112] and the SCL process has been successfully operated for over 300 h in an integrated 25 kWth subpilot unit for the cogeneration of heat and hydrogen with a greater than 99.9% purity

Figure 10. Photo of the OSU high-pressure SCL pilot plant at the NCCC in Alabama for hydrogen generation and CO_2 capture.

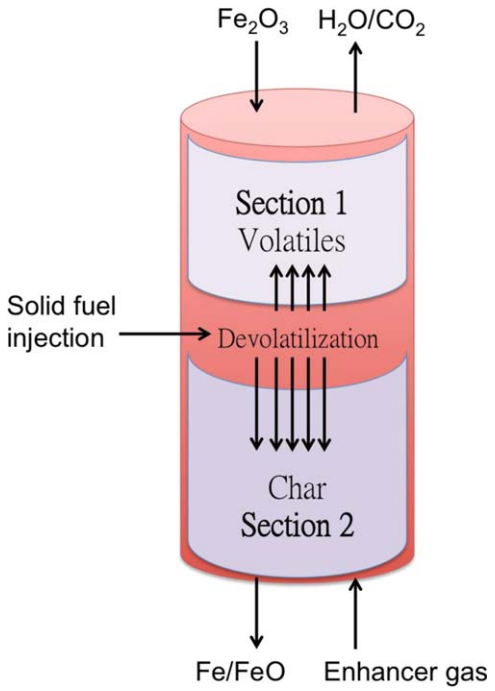

Figure 11. Moving-bed reducer layout for the OSU CDCL process.

with 100% carbon capture and nearly 100% syngas conversion.[113] Figure 9 presents results from a three-day operation of the subpilot unit. It shows steady, continuous, high-purity CO_2 and H_2 generation from the reducer and oxidizer gas outlets, respectively. Analysis of the OSU SCL process has shown that it can reduce the cost of electricity production with CO_2 capture by 11% and the cost of H_2 production by 7–9% over the corresponding baseline cases.[107,108,114]

OSU constructed a pilot-scale SCL demonstration facility processing syngas as a feed from a Kellogg Brown and Root (KBR) transport gasifier at the NCCC in Wilsonville, Alabama. Figure 10 is a photo of the 250-KWth to 3-MWth pilot plant, which is in operation under pressurized conditions (up to 15 atm).

CDCL type A-I process

The CDCL process converts solid fuels, such as coal or biomass, to products such as electricity and/or hydrogen with CO_2 capture.[115,116] Coal is injected into the reducer, and this is divided into two sections, as illustrated in Figure 11. The coal decomposes into volatiles and char in the reducer after it is injected. In the upper section, the volatiles moving upward react with the downward-flowing oxygen carriers. In

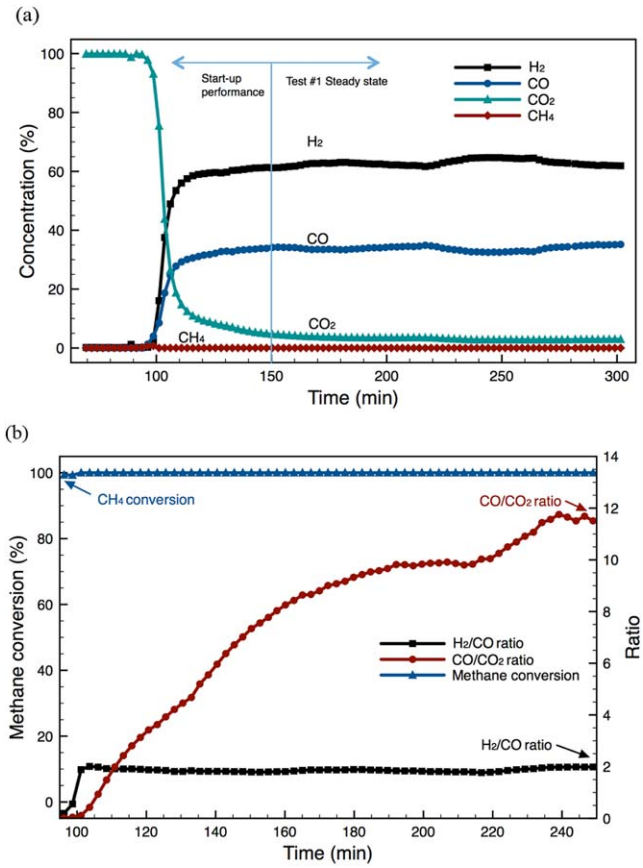

Figure 12. Performance of the OSU shale gas (methane)-to-syngas (STS) subpilot unit operation: (a) syngas compositions and (b) methane conversion and hydrogen-to-carbon monoxide ratios.

the lower section, the slow solid-solid reaction between char and the oxygen carriers is facilitated with an enhancing gas, such as steam and/or CO_2. The enhancer gas gasifies the char, which is then oxidized to CO_2 and H_2O by the oxygen carriers. The moving-bed reducer design ensures full fuel conversion and achieves a high oxygen-carrier conversion. Table 2 summarizes results from various bench unit and subpilot unit tests. A 25-kWth fully integrated subpilot chemical-looping facility with complete zone sealing and nonmechanical valves for gas and solid circulation control has been operated. A successful 200-h continuous subpilot run achieved nearly complete coal conversions to CO_2 and steam with no solid circulation or gas flow issues observed throughout the run.[115] A pilot plant is being constructed by the Babcock and Wilcox Power Generation Group, Inc.

Table 2. Summary of the OSU's Bench and Small Pilot-Scale Unit Testing Results that Use Different Fuels for CO_2 Capture

	Bench scale (2.5 kWth)							Subpilot (25 kWth)		
	Coal volatile		Coal char		Coal			Coal		
Type of fuel	CO, H_2	CH_4	Lignite	Bituminous	PRB	Illinois #6	Anthracite	Metallurgical coke	PRB	Illinois #6
Fuel conversion (%)	99.9	99.8	94.9	95.2	>97	>95	95.5	81	99	70
CO_2 purity (%)	99.9	98.8	99.2	99.1	—	—	97.3	99.85	98	97

[a]PRB: powder river basin sub-bituminous coal.

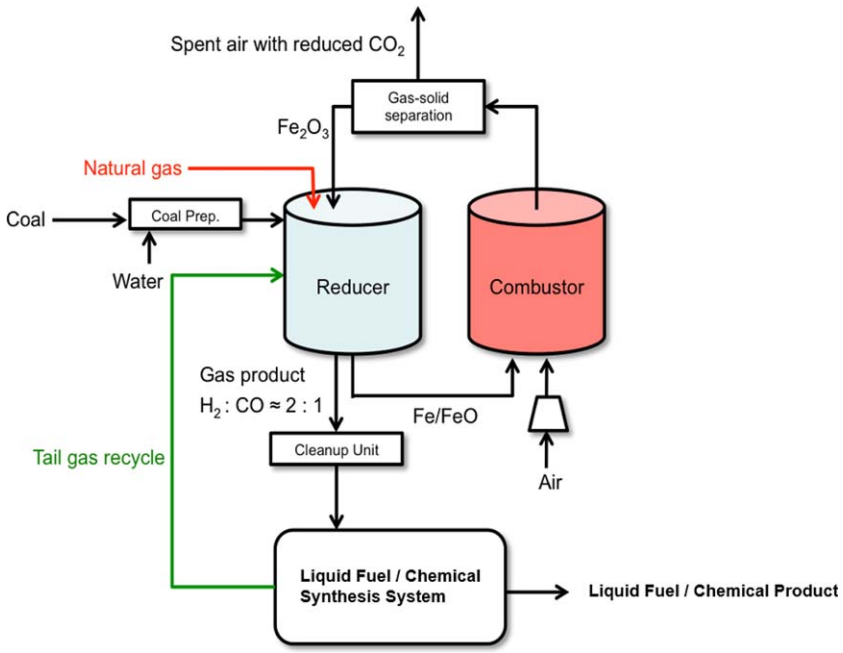

Figure 13. Schematic flow diagram of the chemical-looping gasification process for the liquid fuel synthesis.

The CDCL process can be directed toward electricity production, H_2 production, or a combination of the two products. Comprehensive techno-economic simulations have been reported for the CDCL system.[116,117] The simulation results were derived on the basis of experimental performance parameters.[115] The process economic calculations for the electricity generation case were computed with the methodology and assumptions specified in the DOE baseline report and in the DOE's *Quality Guidelines for Energy System Studies*.[108–111,118] The estimated first-year cost of electricity (COE) for an iron-looping plant with the CDCL technology was 78.4 $/MWh.[117] This value was 33% greater than a base pulverized coal combustion plant without carbon capture ($58.90/MWh) but 22% lower than the first-year cost of electricity of a monoethanolamine plant ($ 100.90/MWh). The percentage increase in COE has been projected to meet the DOE's target of more than 90% CO_2 capture while keeping the increment in COE to less than 35%.

STS and CTS type B-I processes

The STS and CTS processes are more recent developments with similar reactor configurations; hence, both processes are described together. However, the processes vary in the feedstock used, and so different operating schemes are used.

STS Process. The STS chemical-looping process was developed for the production of high-purity syngas from feedstocks, such as shale gas or other gaseous fuels.[67,103] The STS conversion is facilitated in a single step by the donation of a lattice oxygen from an iron-titanium composite metal oxide (ITCMO). The ITCMO circulates in an autothermal loop similar to the SCL and CDCL processes described previously. The STS process is characterized by a cocurrent downward gas-solid moving-bed reducer reactor. The ITCMO conversion is controlled to ensure high CO/CO_2 and H_2/CO ratios in the product syngas and to prevent carbon deposition.

The STS process has been successfully tested in a subpilot-scale moving-bed reactor system with methane as the feedstock.[67] A methane conversion of greater than 99%, a CO/CO_2 molar ratio of about 9:1, and a H_2/CO molar ratio of about 2:1 was observed. Figure 12 shows the CH_4 conversion and gas composition results from the subpilot tests. The techno-economic feasibility of the STS process was compared against an autothermal reformer that converted natural gas to a syngas stream.[67] The performance of the autothermal reformer, which gave a syngas purity of 83% and no electricity production, was reported in a DOE baseline report.[119] The STS process operates at 10 atm and produces a syngas purity of 92% while producing excess electricity that can be used to satisfy parasitic energy requirements. For an equivalent amount of syngas specification (H_2/CO ratio), the chemical-looping system has a higher selectivity. The higher intrinsic selectivity coupled with the lower steam consumption and no molecular oxygen requirement make the STS process a promising alternative to conventional systems.

CTS Process. The CTS chemical-looping process was developed for the production of high-purity syngas from coal or other solid-fuel feedstocks.[103] Figure 13 shows a two-reactor chemical-looping gasification scheme of the CTS process. The CTS process uses a cocurrent contact mode with an oxygen carrier to achieve a high conversion of the carbonaceous fuel. The overall aim is to generate a syngas stream with an appropriate H_2/CO ratio (ca. 2) such that it is suitable for downstream processing to produce liquid fuels and chemicals. To produce a suitable H_2/CO ratio, natural gas, water/steam, or even light hydrocarbons may be introduced together with a coal/solid-fuel feedstock in the reducer. The conventional approach gasifies the fuel to

obtain an H_2/CO ratio that is close to the intrinsic value of the ratio in the fuel used. If a hydrogen-deficient fuel such as coal or biomass is used, the H_2/CO ratio is increased with either the WGS reaction or a separate reforming step such as in the autothermal reactor. The WGS reaction reacts H_2O with the CO in syngas to produce CO_2 and H_2. This increases the H_2/CO ratio of the syngas at the cost of carbon utilization as the CO_2 produced is separated before downstream processing. In cases where an additional reforming step is required, the overall cost of chemical/liquid fuels produced increases because of the increased capital and operational costs.

In the CTS process, coal and iron oxide composite particles flow downward along the reducer. In the reducer, the oxygen carrier partially oxidizes the fuel to syngas, whereas the composite metal oxide as oxygen carrier is reduced. Coal ash and impurities are treated in a similar manner as to those described for the CDCL process. The CTS process eliminates the need for an air separation unit, a WGS reactor, and an acid gas removal unit as compared to the conventional coal-gasification process. This significantly reduces the capital and operational costs for syngas production. The CTS process has been tested successfully on a bench-scale level.

Conclusions: Progress, Challenges, and Future Outlook

In a broad sense, the looping species can be in a gaseous, liquid, or solid form. However, when the feedstock of particular interest is a carbonaceous material, the looping species would mainly be metal oxide based materials in particulate form. The chemical-looping operation embodies all of the elements of particle science and technology including particle synthesis, particle reactivity and mechanical properties, flow stability and contact mechanics, gas-solid reaction, and system engineering. The nature of the reaction path design can be either partial or full oxidation; this enables the development into novel technology platforms and generates a variety of products ranging from electricity and hydrogen to olefins and liquid fuels through process intensification.

Progress

The chemical-looping concept was conceived and practiced as early as the 1900s. Early interest was mainly in the production of hydrogen.[2,3] It was discontinued a short while later until the 1960s to 1970s when it was applied to the generation of synthetic natural gas.[5,6,14] The discontinuity and the shift in interest showed a close connection to the low efficiency of the earlier processes, the limited supply and high prices of the feedstock and/or the low prices of the products. The interest in the chemical-looping concept and its applications resurfaced in the 1980s in light of the interest in enhancing the exergy efficiency in solid fuel combustion and later in the effective capture of CO_2 from carbonaceous fuel.[41,43] Currently, with an abundant supply of shale gas/natural gas in the United States and the necessity of using coal for electricity generation in other countries, the prospect of converting natural gas or coal for combustion and gasification applications with chemical-looping processes in place of the traditional processes has brought a renewed excitement to this technology application.

Challenges

Despite extensive engagement in their development, chemical-looping processes have not been successfully demonstrated commercially to date. The reasons are principally two. The first is concerned with the oxygen carriers, namely, their inadequacy in reactivity and recyclability, physical strength and attrition resistance, and oxygen-carrying capacity. The second is connected with the solid circulatory systems, specifically the lack of design know-how on high-solid loading flows, nonmechanical devices, and gas-solid reactors for achieving high oxygen-carrier conversions. The earlier use of active pure metal oxides or natural mineral metal oxide materials for oxygen carriers did not recognize the importance of the cation and anion diffusion mechanism; associated phase-separation phenomena; metal oxide support, which helps provide lattice vacancies to facilitate the ionic diffusion; and void, cavity, or micropore creations through vacancy migration, agglomeration, and sintering to facilitate molecular pore diffusion. Thus, the reactivity of oxygen carriers could not be maintained for many cycles of the redox reactions. Furthermore, the lack of effective methods in the synthesis of robust oxygen carriers to sustain their morphological variations during the cyclic reactions and their physical stresses during the circulation hampered the utilization of a solid flow system in carrying out the chemical-looping operation. The unsuccessful commercial development and operation of DuPont's chemical-looping butane oxidation process for the production of maleic anhydride in the 1980s and 1990s serves as a reminder of the importance of viability—both of the chemical and physical properties of the metal oxide oxygen carriers in the entire scale-up procedure.

An earlier design of the reducer reactors was based on fixed-bed reactors, whose scaling prospect was limited because of their use in high-temperature switching valves.[2,3] For a large-scale solid circulation system, the control of a solid circulation rate cannot be made without nonmechanical valves, and the operating principles for nonmechanical valves, such as L valves, were not known until the 1970s and 1980s.[120] Thus, earlier efforts on the scale-up of high-temperature, continuous solid reactive circulation systems were also severely limited in chemical-looping applications. Furthermore, the early design of the solid circulatory system neglected the consideration of the thermodynamic properties of the metal oxides, which are manifested in the behavior of their phase diagram. The phase diagram of the metal oxide illustrates the relationship of the specific oxidation states of the metal oxide and their equilibrium oxidized gas compositions. The gas-solid contact pattern in the reduction reactors could not be optimally configured without the recognition of such phase diagrams.

Future outlook

Extensive recent research and development efforts have been focused on the design and synthesis of oxygen-carrying particles and the understanding of the ionic transport phenomena of metal oxide materials in the redox reactions. Much progress has been made in the science and engineering of these materials, including the oxygen uncoupling materials that release molecular oxygen and the complex ferrites and perovskite materials that enhance the reaction kinetics

through augmentation of electron and/or ionic transfer. The work accomplished from this progress has significantly remedied the earlier causes of failure indicated previously.

The configuration of the gas-solid contact pattern for the reduction reactor design by consideration of the metal oxide phase diagram can contribute to the achievement of a high oxygen donor capacity for the oxygen carrier and, hence, reduce the solid circulation rate required for given feedstock loading condition. With thermodynamic properties of complex metal oxide composite materials becoming available, reactors can be now better designed for high oxygen-carrier conversions. Fluidized beds and moving beds are two main types of reactors considered for large-scale reducer operations. Much progress has been made in the operation of fluidized-bed reducers with ongoing large pilot demonstrations. Although either type of reactor, in a single or an assembly reactor arrangement, can achieve the same reactant conversion, process economics eventually come into play in the determination of the optimum reactor configuration. In this regard, because of the use of a single reactor with a fixed reactor volume and feedstock loading, the analysis indicates that higher gas and solid conversions can be achieved with a moving-bed reducer compared to that with a fluidized-bed reducer. This analysis can be substantiated by the experimental data on the reactant conversion and product generation for both full oxidation and partial oxidation conditions. For example, with ilmenite as the oxygen carrier, the typical extent of coal conversions for full oxidation as reported with fluidized-bed reducers was 70–80%,[121,122] whereas for the moving-bed reducers, they typically were greater than 90%.[115,123,124] For partial oxidation with fluidized-bed reducers, the typical carbon efficiency of methane conversion to syngas with nickel oxides was 50–60%,[125,126] and that with ilmenite was about 60%.[127] With ITCMOs with moving-bed reducers, the typical carbon efficiency of methane conversion to syngas was greater than 85%.[67]

The concept of chemical looping has existed for over a century. Recently, there has been a renewed interest in developing and commercializing chemical-looping technologies because of the potential of generating valuable commodities with inherent carbon capture. From the development of chemical-looping concepts to the demonstration of pilot-scale units, global research from academia and industry has advanced the status of chemical looping. OSU has developed a chemical-looping technology platform that comprises six processes that generate a variety of products, including electricity, syngas, hydrogen, chemicals, and liquid fuels, with CO_2 capture. With extensive technological advancements in solid handling, particle synthesis, and reactor design, the outlook of chemical-looping technology is promising.

Final remarks

Overall, for chemical-looping combustion and gasification applications, the solid circulating systems with nonmechanical devices and zone seals are of little commercial risk and are scalable. The development of a large-scale circulating system or a CFB system that processes massive solid flows well, exceeding that of conventional FCC systems, is challenging but attainable. The key challenge to the commercialization of the chemical-looping processes and timing for its deployment is, however, on the robustness and the economic readiness of the oxygen carriers in their long-term viable operation. The "long term" refers to the timescale on the order of several months, whereas the "viable" refers to the chemical (e.g., oxygen-carrying capacity and recyclability) and physical (e.g., attrition resistance and flowability) properties that can be sustained in this long-term timescale. With much known now and continued extensive worldwide research and development efforts on oxygen carriers, challenges to meeting such stringent property requirements should not be unsurmountable. It is projected that the first commercial chemical-looping process will emerge from shale gas/natural gas based applications. The prospect of its timing may likely be in the near future.

Acknowledgments

The work was supported in part by the C. John Easton Professorship endowed funds at OSU. The helpful assistance of Mandar Kathe, Dikai Xu, and William Wang during the preparation of this article is gratefully acknowledged.

Literature Cited

1. Ishida M, Zheng D, Akehata T. Evaluation of a chemical-looping combustion power-generation system by graphic exergy analysis. *Energy*. 1987;12:147–154.
2. Messerschmitt A. Process for producing hydrogen. US patent 971,206. 1910.
3. Lane H. Process for the production of hydrogen. US patent 1,078,686. 1913.
4. Fan LS. *Chemical Looping Systems for Fossil Energy Conversions*. Hoboken, NJ: Wiley; 2010.
5. Knoche KF, Richter H. Improvement of reversibility of combustion processes. *Brennstoff-Warme-Kraft*. 1968;20:205.
6. Richter H, Knoche K. Reversibility of combustion processes. In: Gaggioli RA, ed. *Efficiency and Costing*. Washington, DC: American Chemical Society; 1983:71–86. ACS Symposium Series 235.
7. Bhavsar S, Najera M, Solunke R, Veser G. Chemical looping: to combustion and beyond. *Catal Today*. 2014;228:96–105.
8. Fan LS, Zeng L, Wang W, Luo S. Chemical-looping processes for CO_2 capture and carbonaceous fuel conversion—prospect and opportunity. *Energy Environ Sci*. 2012;5:7254–7280.
9. Hurst S. Production of hydrogen by the steam-iron method. *J Am Oil Chem Soc*. 1939;16:29–36.
10. Gasior S, Forney A, Field J, Bienstock D, Benson H. *Production of Synthesis Gas and Hydrogen by the Steam-Iron Process*. Washington, DC: US Department of the Interior, Bureau of Mines; 1961. Report of investigations 5911.
11. Teed PL. *The Chemistry and Manufacture of Hydrogen*. New York, NY: Longmans, Green and Co.; 1919.
12. Lewis WK, Gilliland ER. Production of pure carbon dioxide. US patent 2,665,971. 1954.
13. Lewis WK, Gilliland ER. Production of pure carbon dioxide. US patent 2,665,972. 1954.

14. Institute of Gas Technology. *Development of the Steam-Iron Process for Hydrogen Production*. Washington, DC: US Department of Energy; 1979. Report EF-77-C-01-2435.
15. Dobbyn RC, Dobbyn RC, Ondik HM, et al. *Evaluation of the Performance of Materials and Components Used in the CO_2 Acceptor Process Gasification Pilot Plant*. Washington, DC: US Department of Energy; 1978. Report DOE-ET-10253-T1.
16. Lin SY, Suzuki Y, Hatano H, Harada M. A new method (HyP-RING) for producing hydrogen from coals. Paper presented at: 10th International Conference on Coal Science; Taiyuan, China; 1999.
17. Lin, SY, Harada M, Suzuki Y, Hatano H. Process analysis for hydrogen production by reaction integrated novel gasification (Hypr-ring). *Energy Convers Manag*. 2005; 46:869–880.
18. Keller GE, Bhasin MM. Synthesis of ethylene via oxidative coupling of methane. *J Catal*. 1982;73:9–19.
19. Jones CA, Leonard JJ, Sofranko JA. The oxidative conversion of methane to higher hydrocarbons over alkali-promoted $MnSiO_2$. *J Catal*. 1987;103:311–319.
20. Jones CA, Leonard JJ, Sofranko JA. Fuels for the future: remote gas conversion. *Energy Fuels*. 1987;1:12–16.
21. Contractor RM. Dupont's CFB technology for maleic anhydride. *Chem Eng Sci*. 1999;54:5627–5632.
22. Dudukovic MP. Frontiers in reactor engineering. *Science*. 2009;325:698–701.
23. Otsuka K, Wang Y, Sunada E, Yamanaka I. Direct partial oxidation of methane to synthesis gas by cerium oxide. *J Catal*. 1998;175:152–160.
24. Wang S, Kobayashi T, Dokiya M, Hashimoto T. Electrical and ionic conductivity of Gd-doped ceria. *J Electrochem Soc*. 2000;147:3606–3609.
25. Gupta A, Hegde M, Priolkar K, Waghmare U, Sarode P, Emura S. Structural investigation of activated lattice oxygen in $Ce_{1-x}Sn_xO_2$ and $Ce_{1-x-y}Sn_xPd_yO_{2-\delta}$ by EXAFS and DFT calculation. *Chem Mater*. 2009;21:5836–5847.
26. Salazar-Villalpando MD, Berry DA, Cugini A. Role of lattice oxygen in the partial oxidation of methane over Rh/zirconia-doped ceria. Isotopic studies. *Int J Hydrogen Energy*. 2010;36:1998–2003.
27. Bhavsar S, Veser G. Chemical looping beyond combustion: production of synthesis gas via chemical looping partial oxidation of methane. *RSC Adv*. 2014;4:47254–47267.
28. Steinfeld A, Kuhn P, Karni J. High-temperature solar thermochemistry—production of iron and synthesis gas by Fe_3O_4-reduction with methane. *Energy*. 1993;18:239–249.
29. Fletcher EA. Solar thermal processing: a review. *J Sol Energy Eng*. 2001;123:63–74.
30. Steinfeld A. Solar thermochemical production of hydrogen—a review. *Sol Energy*. 2005;78:603–615.
31. Muhich CL, Evanko BW, Weston KC, et al. Efficient generation of H_2 by splitting water with an isothermal redox cycle. *Science*. 2013;341:540–542.
32. Ströhle J, Orth M, Epple B. Design and operation of a 1MWth chemical looping plant. *Appl Energy*. 2014;113: 1490–1495.
33. Tong A, Bayham S, Kathe M, Zeng L, Luo S, Fan LS. Iron-based syngas chemical looping process and coal-direct chemical looping process development at Ohio State University. *Appl Energy*. 2014;113:1836–1845.
34. Arias B, Diego M, Abanades J, et al. Demonstration of steady state CO_2 capture in a 1.7 MWth calcium looping pilot. *Int J Greenhouse Gas Con*. 2013;18:237–245.
35. Chang MH, Huang CM, Liu WH, et al. Design and experimental investigation of calcium looping process for 3-kWth and 1.9-MWth facilities. *Chem Eng Technol*. 2013;36:1525–1532.
36. Wang W, Ramkumar S, Li S, et al. Subpilot demonstration of the carbonation-calcination reaction (CCR) process: high-temperature CO_2 and sulfur capture from coal-fired power plants. *Ind Eng Chem Res*. 2010;49: 5094–5101.
37. Kremer J, Galloy A, Strohle J, Epple. Continuous CO_2 capture in a 1-MWth carbonate looping pilot plant. *Chem Eng Technol*. 2013;36:1518–1524.
38. Hossain MM, de Lasa HI. CLC for inherent CO_2 separations—a review. *Chem Eng Sci*. 2008;63:4433–4451.
39. Jin HG, Ishida M. A new type of coal gas fueled chemical-looping combustion. *Fuel*. 2004;83:2411–2417.
40. Johansson E, Mattisson T, Lyngfelt A, Thunman H. Combustion of syngas and natural gas in a 300W chemical-looping combustor. *Chem Eng Res Des*. 2006; 84:819–827.
41. Ishida M, Jin HG. A new advanced power-generation system using chemical-looping combustion. *Energy*. 1994;19:415–422.
42. Dewulf J, Van Langenhove H, Muys B, et al. Exergy: its potential and limitations in environmental science and technology. *Environ Sci Technol*. 2008;42:2221–2232.
43. Anheden M, Svedberg G. Exergy analysis of chemical-looping combustion systems. *Energy Convers. Manag*. 1998;39:1967–1980.
44. Blockstein DE, Shockley MA. *Energy for a Sustainable and Secure Future: A Report of the Sixth National Conference on Science, Policy and the Environment*. Washington, DC: National Council for Science and the Environment; 2006.
45. Chatel-Pelage F, Varagani R, Pranda P, et al. Applications of oxygen for NO_x control and CO_2 capture in coal-fired power plants. *Therm Sci*. 2006;10:119–142.
46. Wang M, Lawal A, Stephenson P, Sidders J, Ramshaw C. Post-combustion CO_2 capture with chemical absorption: a state-of-the-art review. *Chem Eng Res Des*. 2011; 89:1609–1624.
47. White CM, Strazisar BR, Granite EJ, Hoffman JS, Pennline HW. Separation and capture of CO_2 from large stationary sources and sequestration in geological formations—coalbeds and deep saline aquifers. *J Air Waste Manag Assoc*. 2003;53:645–715.
48. Aaron D, Tsouris C. Separation of CO_2 from flue gas: a review. *Sep Sci Technol*. 2005;40:321–348.
49. Iyer MV, Gupta H, Sakadjian BB, Fan LS. Multicyclic study on the simultaneous carbonation and sulfation of high-reactivity CaO. *Ind Eng Chem Res*. 2004;43:3939–3947.
50. Kotas TJ. *The Exergy Method of Thermal Plant Analysis*. Oxford, UK: Butterworth-Heinemann; 1985.

51. Tsutsumi A. Exergy recuperative gasification technology for hydrogen and power co-production. Paper presented at: 231st ACS National Meeting; Atlanta, GA; 2006.
52. Adánez J, de Diego LF, García-Labiano F, Gayán P, Abad A, Palacios J. Selection of oxygen carriers for chemical-looping combustion. *Energy Fuels.* 2004;18: 371–377.
53. Adánez J, Abad A, Garcia-Labiano F, Gayan P, de Diego LF. Progress in chemical-looping combustion and reforming technologies. *Prog Energy Combust Sci.* 2012; 38:215–282.
54. Xu D, Luo S, Zeng L, LS. Fan. Unpublished work. 2014.
55. Luis F, Adánez J, Gayán P, Abad A, Corbella BM, Palacios JM. Development of Cu-based oxygen carriers for chemical-looping combustion. *Fuel.* 2004;83:1749–1757.
56. Lee JB, Park CS, Choi SI, Song YW, Kim YH, Yang HS. Redox characteristics of various kinds of oxygen carriers for hydrogen fueled chemical-looping combustion. *J Ind Eng Chem.* 2005;11:96–102.
57. Song Q, Xiao R, Deng Z, Zheng W, Shen L, Xiao J. Multicycle study on chemical-looping combustion of simulated coal gas with a $CaSO_4$ oxygen carrier in a fluidized bed reactor. *Energy Fuels.* 2008;22:3661–3672.
58. Li F, Luo S, Sun Z, Fan LS. Role of metal oxide support in redox reactions of iron oxide for chemical looping applications: experiments and density functional theory calculations. *Energy Environ Sci.* 2011;4:3661–3667.
59. Edstrom J. Solid-state diffusion in the reduction of hematite. *Jernkontorets Ann.* 1957;141:809–836.
60. Rubel A, Liu K, Neathery J, Taulbee D. Oxygen carriers for chemical looping combustion of solid fuels. *Fuel.* 2009;88:876–884.
61. Adánez J, De Diego LF, García-Labiano F, Gayán P, Abad A, Palacios JM. Selection of oxygen carriers for chemical-looping combustion. *Energy Fuels.* 2004;18: 371–377.
62. Yu FC, Phalak N, Sun Z, Fan LS. Activation strategies for calcium-based sorbents for CO_2 capture: a perspective. *Ind Eng Chem Res.* 2011;51:2133–2142.
63. Leion H, Lyngfelt A, Johansson M, Jerndal E, Mattisson T. The use of ilmenite as an oxygen carrier in chemical-looping combustion. *Chem Eng Res Des.* 2008;86:1017–1026.
64. Cuadrat A, Abad A, Adánez J, de Diego LF, García-Labiano F, Gayán P. Behavior of ilmenite as oxygen carrier in chemical-looping combustion. *Fuel Process Technol.* 2012;94:101–112.
65. Qin L, Majumder A, Fan JA, Kopechek D, Fan LS. Evolution of nanoscale morphology in single and binary metal oxide microparticles during reduction and oxidation processes. *J Mater Chem A.* 2014;2:17511–17520.
66. Zhao C, Li Y, Zhou J, et al. Large-scale synthesis of bicrystalline ZnO nanowire arrays by thermal oxidation of zinc film: growth mechanism and high-performance field emission. *Cryst Growth Des.* 2013;13:2897–2905.
67. Luo S, Zeng L, Xu D, et al. Shale gas-to-syngas chemical looping process for stable shale gas conversion to high purity syngas with H_2:CO ratio of 2:1. *Energy Environ Sci.* 2014;7:4104–4117.
68. Sun Z, Zhou Q, Fan LS. Formation of core-shell structured composite microparticles via cyclic gas-solid reactions. *Langmuir.* 2013;29:12520–12529.
69. Kuo YL, Hsu WM, Chiu PC, Tseng YH, Ku Y. Assessment of redox behavior of nickel ferrite as oxygen carriers for chemical looping process. *Ceram Int.* 2013;39: 5459–5465.
70. Qin L, Fan J. A., Sun Z, Fan LS. Nano/micro scale redox phenomena of metals/oxides and other chemical and electrical characteristics. Presented at: 248th ACS National Meeting; San Francisco, CA; 2014.
71. Mattisson T, Leion H, Lyngfelt A. Chemical-looping with oxygen uncoupling using CuO/ZrO_2 with petroleum coke. *Fuel.* 2009;88:683–690.
72. Zhu Y, Mimura K, Isshiki M. Oxidation mechanism of Cu_2O to CuO at 600–1050°C. *Oxid Met.* 2004;62:207–222.
73. Azimi G, Ryden M, Leion H, Mattisson T, Lyngfelt A. $(Mn_zFe_{1-z})_yO_x$ combined oxides as oxygen carrier for chemical-looping with oxygen uncoupling. *AIChE J.* 2012;59:582–588.
74. Azimi G, Leion H, Ryden M, Mattisson T, Lyngfelt A. Investigation of different Mn-Fe oxides as oxygen carrier for chemical-looping with oxygen uncoupling (CLOU). *Energy Fuels.* 2013;27:367–377.
75. Azad A, Hedayati A, Ryden M, Leion H, Mattisson T. Examining the Cu-Mn-O spinel system as an oxygen carrier in chemical looping combustion. *Energy Technol.* 2013;1:59–69.
76. Dai X, Wu Q, Li R, Yu C, Hao Z. Hydrogen production from a combination of the water-gas shift and redox cycle process of methane partial oxidation via lattice oxygen over $LaFeO_3$ perovskite catalyst. *J Phys Chem B.* 2006;110:25856–25862.
77. Galinsky NL, Huang Y, Shafiefarhood A, Li F. Iron oxide with facilitated O^{2-} transport for facile fuel oxidation and CO_2 capture in a chemical looping scheme. *ACS Sustain Chem Eng.* 2013;1:364–373.
78. Mihai O, Chen D, Holmen A. Catalytic consequence of oxygen of lanthanum ferrite perovskite in chemical looping reforming of methane. *Ind Eng Chem Res.* 2011;50: 2613–2621.
79. Carter S, Selcuk A, Chater RJ, Kajda J, Kilner JA, Stelle BCH. Oxygen transport in selected nonstoichiometric perovskite-structure oxides. *Solid State Ionics.* 1992;53: 597–605.
80. Hallberg P, Jing D, Ryden M, Mattisson T, Lyngfelt A. Chemical looping combustion and chemical looping with oxygen uncoupling experiments in a batch reactor using spray-dried $CaMn_{1-x}M_xO_{3-\delta}$ (M = Ti, Fe, Mg) particles as oxygen carriers. *Energy Fuels.* 2013;27: 1473–1481.
81. Arjmand M, Hedayati A, Azad AM, Leion H, Ryden M, Mattisson T. $Ca_xLa_{1-x}Mn_{1-y}M_yO_{3-\delta}$ (M = Mg, Ti, Fe, or Cu) as oxygen carriers for chemical-looping with oxygen uncoupling (CLOU). *Energy Fuels.* 2013;27:4097–4107.
82. Dai X, Li R, Yu C, Hao Z. Unsteady-state direct partial oxidation of methane to synthesis gas in a fixed-bed reactor using $AFeO_3$ (A=La, Nd, Eu) perovskite-type oxides as oxygen storage. *J Phys Chem B.* 2006;110: 22525–22531.

83. Nalbandian L, Evdou A, Zaspalis V. $La_{1-x}Sr_xM_yFe_{1-y}O_{3-z}$ perovskites as oxygen-carrier materials for chemical-looping reforming. *Int J Hydrogen Energy* 2011;36: 6657–6670.
84. Thursfield A, Murugan A, Franca R, Metcalfe IS. Chemical looping and oxygen permeable ceramic membranes for hydrogen production— a review. *Energy Environ Sci*. 2012;5:7421–7459.
85. Kimball E, Hamers HP, Cobden P, Gallucci F, van Sint Annaland M. Operation of fixed-bed chemical looping combustion. *Energy Procedia*. 2013;37:575–579.
86. Hamers HP, Romano MC, Spallina V, Chiesa P, Gallucci F, van Sint Annaland M. Comparison on process efficiency for CLC of syngas operated in packed bed and fluidized bed reactors. *Int J Greenhouse Gas Con*. 2014;28:65–78.
87. Noorman S, van Sint Annaland M, Kuipers J. Experimental validation of packed bed chemical-looping combustion. *Chem Eng Sci*. 2010;65:92–97.
88. Hamers HP, Gallucci F, Cobden P, Kimball E, van Sint Annaland M. A novel reactor configuration for packed bed chemical-looping combustion of syngas. *Int J Greenhouse Gas Con*. 2013;16:1–12.
89. Mattisson T, Johansson M, Lyngfelt A. The use of NiO as an oxygen carrier in chemical-looping combustion. *Fuel*. 2006;85:736–747.
90. Cho P, Mattisson T, Lyngfelt A. Comparison of iron-, nickel-, copper- and manganese-based oxygen carriers for chemical-looping combustion. *Fuel*. 2004;83:1215–1225.
91. Abad A, Mattisson T, Lyngfelt A, Johansson M. The use of iron oxide as oxygen carrier in a chemical-looping reactor. *Fuel*. 2007;86:1021–1035.
92. Berguerand N, Lyngfelt A. Design and operation of a 10 kWth chemical-looping combustor for solid fuels—Testing with South African coal. *Fuel*. 2008;87:2713–2726.
93. Berguerand N, Lyngfelt A. The use of petroleum coke as fuel in a 10 kWth chemical-looping combustor. *Int J Greenhouse Gas Con*. 2008;2:169–179.
94. de Diego LF, Garcia-Labiano F, Gayan P, Celaya J, Palacios JM, Adanez J. Operation of a 10 KWth chemical-looping combustor during 200 h with a CuO-Al_2O_3 oxygen carrier. *Fuel*. 2007;86:1036–1045.
95. Ryu HJ, Seo Y, Jin GT. Development of chemical-looping combustion technology: long-term operation of a 50 KWth chemical-looping combustor with Ni- and Co-based oxygen carrier particles. In: *Proceedings of the 12th Regional Symposium on Chemical Engineering*. Hanoi, Vietnam: RSCE; 2005.
96. Pröll T, Kolbitsch P, Bolhàr-Nordenkampf J, Hofbauer H. A novel dual circulating fluidized bed (DCFB) system for chemical looping process. *AIChE J*. 2009;55:3255–3266.
97. Shen L, Wu J, Xiao J. Experiments on chemical looping combustion of coal with a NiO based oxygen carrier. *Combust Flame*. 2009;156:721–728.
98. Shen L, Wu J, Xiao J, Song Q, Xiao R. Chemical-looping combustion of biomass in a 10 KWth reactor with iron oxide as an oxygen carrier. *Energy Fuels*. 2009;23: 2498–2505.
99. Gu H, Shen L, Xiao J, Zhang S, Song T. Chemical looping combustion of biomass/coal with natural iron ore as oxygen carrier in a continuous reactor. *Energy Fuels*. 2011;25:446–455.
100. Cao Y, Pan WP. Investigation of chemical looping combustion by solid fuels. 1. Process analysis. *Energy Fuels*. 2006;20:1836–1844.
101. Eyring EM, Konya G, Lighty JS, Sahir AH, Sarofim AF, Whitty K. Chemical looping with copper oxide as carrier and coal as fuel. *Oil Gas Sci Technol*. 2011;66: 209–221.
102. Li F, Zeng L, Velazquez-Vargas, LG, Yoscovits Z, Fan LS. Syngas chemical looping gasification process: bench-scale studies and reactor simulations. *AIChE J*. 2010;56:2186–2199.
103. Fan LS, Luo S, Zeng L. Methods for fuel conversion. PCT application PCT/US2014/014877. 2013.
104. Ramkumar S, Fan LS. Calcium looping process (CLP) for enhanced noncatalytic hydrogen production with integrated carbon dioxide capture. *Energy Fuels*. 2010; 24:4408–4418.
105. Ramkumar S, Fan LS. Calcium looping process (CLP) for enhanced noncatalytic hydrogen production with integrated carbon dioxide capture. *Energy Fuels*. 2010; 24:4408–4418.
106. Connell D, Lewandowski D, Ramkumar S, Phalak N, Statnick R, Fan LS. Process simulation and economic analysis of the calcium looping process (CLP) for hydrogen and electricity production from coal and natural gas. *Fuel*. 2013;105:383–396.
107. Rath L. *Assessment of Hydrogen Production with CO_2 Capture. Volume 1: Baseline State-of-the-Art Plants*. Washington, DC: US Department of Energy; 2010. Report DOE/NETL-2010/1434.
108. Black J. *Cost and Performance Baseline for Fossil Energy Power Plants, Volume 1: Bituminous Coal and Natural Gas to Electricity*. Washington, DC: US Department of Energy; 2010. Report DOE/NETL-2010/1397.
109. Turner MJ. *Quality Guidelines for Energy System Studies: Capital Cost Scaling Methodology*. Washington, DC: US Department of Energy; 2013. Report DOE/NETL-341/013113.
110. Chou V, Keairns D, Turner M, Woods M, Zoelle A. *Quality Guidelines for Energy System Studies: Process Modeling Design Parameters*. Washington, DC: US Department of Energy; 2014. Report DOE/NETL-341/051314.
111. Herron S, Myles P. *Quality Guidelines for Energy System Studies: CO_2 Impurity Design Parameters*. Washington, DC: US Department of Energy; 2013. Report DOE/NETL-341/011212.
112. Zhou Q, Zeng L, Fan LS. Syngas chemical looping process: dynamic modeling of a moving bed reducer. *AIChE J*. 2013;59:3432–3443.
113. Tong A, Sridhar D, Sun Z, et al. Continuous high purity hydrogen generation from a syngas chemical looping 25kWth subpilot unit with 100% carbon capture. *Fuel*. 2012;103:495–505.
114. Li F, Zeng L, Fan LS. Techno-economic analysis of coal-based hydrogen and electricity cogeneration processes with CO_2 capture. *Ind Eng Chem Res*. 2010;49: 11018–11028.

115. Bayham S, Kim H, Wang D, et al. Iron-based coal direct chemical looping combustion process: 200-h continuous operation of a 25-kWth subpilot unit. *Energy Fuels*. 2013;27:1347–1356.
116. Zeng L, He F, Li F, Fan LS. Coal-direct chemical looping gasification for hydrogen production: reactor modeling and process simulation. *Energy Fuels*. 2012;26: 3680–3690.
117. Connell DP, Zeng L, Fan LS, Lewandowski DA, Statnick RM. Process simulation of iron-based chemical looping schemes with CO_2 capture for hydrogen and electricity production from coal. Presented at: 29th Annual International Pittsburgh Coal Conference; Pittsburgh, PA; 2012.
118. Black J. *Cost and Performance Baseline for Fossil Energy Power Plants, Volume 3: Low Rank Coal and Natural Gas to Electricity*. Washington, DC: US Department of Energy; 2011. Report DOE/NETL-2010/1399.
119. Goellner JF, Kuehn NJ, Shah V, White CW III, Woods MC. *Baseline Analysis of Crude Methanol Production from Coal and Natural Gas*. Washington, DC: US Department of Energy; 2014. Report DOE/NETL-341/0131114.
120. Knowlton T, Hirsan I. L-valves characterized for solids flow. *Hydrocarbon Process*. 1978;57:149–156.
121. Leion H, Mattisson T, Lyngfelt A. Solid fuels in chemical-looping combustion. *Int J Greenhouse Gas Con*. 2008;2:180–193.
122. Cuadrat A, Abad A, García-Labiano F, Gayán P, De Diego L, Adánez J. The use of ilmenite as oxygen-carrier in a 500Wth chemical-looping coal combustion unit. *Int J Greenhouse Gas Con*. 2011;5:1630–1642.
123. Luo S, Bayham S, Zeng L, et al. Conversion of metallurgical coke and coal using a coal direct chemical looping (CDCL) moving bed reactor. *Appl Energy*. 2014;118:300–308.
124. Kim HR, Wang D, Zeng L, et al. Coal direct chemical looping combustion process: design and operation of a 25-kWth subpilot unit. *Fuel*. 2013;108:370–384.
125. Rydén M, Lyngfelt A, Mattisson T. CLC and chemical-looping reforming in a circulating fluidized-bed reactor using Ni-based oxygen carriers. *Energy Fuels*. 2008;22: 2585–2597.
126. de Diego LF, Ortiz M, García-Labiano F, Adánez J, Abad A, Gayán P. Synthesis gas generation by chemical-looping reforming using a Ni-based oxygen carrier. *Energy Procedia*. 2009;1:3–10.
127. Xu D, Hsieh TL, Tong A, Fan LS. Unpublished data. 2014.